~

Chapter Four

Modeling and Design

~

This chapter describes how, utilizing the technology described in previous chapters, a fuel cell scooter may be designed. It leads from an analysis of performance requirements to a vehicle model to a systems design of the fuel cell stack and auxiliary systems. The model uses basic assumptions to obtain an overall measure of performance; parasitic power is a linear function of gross power, and conservative assumptions are made where data is poorly known.

Two additional options for improved performance and reduced cost, respectively, are considered: operation of the fuel cell at 3 atm pressure, and hybridization with peaking power batteries.

A different kind of scooter – a zinc-air battery-powered alternative – is considered as well because electric scooter manufacturers and researchers in Taiwan are extremely interested in this technology

4.1 Performance requirements

Despite the attraction they offer in the form of zero emissions, battery-powered electric vehicles have failed to capture significant market shares because they are inconvenient to recharge, and because they simply do not match the performance of existing alternatives. The important performance criteria are vehicle range before refueling, power, cost, and to a lesser extent vehicle weight.

The performance characteristics of a few sample vehicles with similar power needs are summarized here as a baseline for the fuel cell scooter; they range from ordinary gasoline scooters to prototype electric scooters to a much heavier demonstration fuel cell - powered golf cart which is included because it is virtually the only PEM fuel cell vehicle designed at the 4-6 kW power output level.

Note that the motor power quoted here is the mechanical power generated; battery or fuel cell output will typically be larger by a factor of 30% due to drivetrain losses.

Table 4.1. Performance of various vehicles of about 5 kW power

Vehicle	Fuel cell electric golf cart	Battery-powered electric scooter (NiCd battery)	Medium-sized two-stroke scooter	Battery-powered electric scooter (lead-acid)
name	Schatz "Personal Utility Vehicle"	Honda CUV ES	Honda Dio	Taiwan ITRI ZES-2000
maximum motor power	1.5 kW (4.0 kW fuel cell)	3.2 kW	5 kW	3.4 kW
range at 30 km/h cruise	24 km	35 km	240 km (5 L tank)	60 km
fuel efficiency at 30 km/h cruise	96 mpge	1000 mpge (46.2 km/kWh)	116 mpg	1300 mpge (60 km/kWh)
acceleration	–	0-200 m in 17.3 seconds	~0-50 m in 6 seconds	0-30 m in 4.5 seconds
maximum speed	20 km/h	60 km/h	~70 km/h	50 km/h
charging time	2 minute cylinder refilling	8 hours full recharge	5 minute gasoline refill	8 hours full recharge
hill climbing	–	–	–	15 km/h at 10° slope
curb weight	380 kg	130 kg	68 kg	105 kg

Taiwan data is from reports published by the Industrial Technology Research Institute[1]. Honda vehicle data are from a Society of Automotive Engineers of Japan paper and a paper published by the ITRI.[2,3] The Schatz Energy Research Center's Personal Utility Vehicle was documented in a 1998 Fuel Cell Seminar abstract, and the weight was from a data sheet for that E-Z Go 4Caddy electric golf cart.[4,5]

Performance measurements marked with tildes were for 50 cc scooters similar to the Dio as data were not directly available.

"curb weight" is the mass of the vehicle without passengers or cargo.

The unusual acceleration measurement (time required to cover a given distance) is a standard for scooters in Asia.

Note that the Dio's 5 kW engine is at the high end of 50 cc vehicles. Many 50 cc scooters have powers of 2-4 kW, while 125 cc scooters produce 6-9 kW of power.

"mpge" (miles per gallon equivalent) fuel economies for the non-combustion vehicles were

calculated by taking the total energy stored – whether as chemical energy in a battery or in terms of hydrogen lower heating value – and calculating how many gallons of gasoline would have to be burned to produce the same amount of heating value energy. This "on-vehicle" fuel economy is slightly misleading in that hydrogen and batteries tend to be higher grade carriers of energy; that is, it would take a large amount of energy from burned petroleum to store the same energy in hydrogen or battery form. Later wells-to-wheels fuel efficiency calculations will take into account the conversion losses.

Nakazawa *et al* claim that the Honda CUV-ES's 35 km range under an urban driving cycle is "sufficient for practical use."[2] Researchers from Taiwan's ITRI (Industrial Technology Research Institute) also claim that daily driving ranges are less than 25 km 68% of the time, and 70% of the daily driving *time* is less than one and a half hours.[6] But, as a point of comparison, a gasoline scooter of similar power (i.e. one with 50 cc displacement) achieves quadruple the range of even the best electric scooters when being driven at a steady speed of 30 km/h. A 35 km range may be enough for use, but electric scooters will never replace a third of two-stroke scooters if their competitors have four times the range with quicker refueling. A more reasonable set of requirements would be to preserve the same minimum acceleration characteristics, but to require that the range be at least 200 km. A range of over 240 km like the Dio is optimal, but probably not necessary and expensive in terms of dollars and volume.

The power of 4-6 kW is relatively high for a lightweight and small vehicle like the scooter, but this is due to the way in which scooters are driven under typical urban conditions. Bursts of rapid acceleration are used to dodge in between larger vehicles in congested traffic, and quick starts are often required when red lights turn green. Frequent decelerations and stops are needed in the city, and scooters are not often taken out on the highway for prolonged high-speed driving. Basically,

average speeds and average power are low, but peak power is high.

Mass is an important consideration too; a curb weight of approximately 130 kg approaches the limits of manageability for parking and unpowered handling.[7] Thus, the minimum requirements for the fuel cell scooter should be:

Table 4.2. Fuel cell scooter performance requirements

Specification	Fuel cell scooter
max motor power output	4-6 kW
range before refueling at 30 km/h cruising speed	200 km
fuel efficiency	> 100 mpge
acceleration	0-30 m in less than 5 seconds
speed on 15° slope	10 km/h
speed on 12° slope	18 km/h
maximum speed	60 km/h
maximum curb weight	140 kg

The slope climbing, acceleration, and maximum speed requirements are based on a Taiwan research lab electric scooter proposal, which in turn was based on surveys of scooter users.[8] (As a comparison point for the speed on inclines, San Francisco's Lombard Street wends up a hill with a 40°slope, although the twisting road itself is limited to 21°).

A broader list of electric scooters that are being developed now is included in Appendix A.

4.2 Vehicle modeling

Essentially, the purpose of vehicle modeling is to convert input parameters (performance measurements like desired range, driving cycle that must be sustained, and types of power and storage components) into the output parameters of curb weight, size of engine required, heating system design, cost, and convenience. The process is iterative; for example, the size of the cooling system is a function of the average vehicle power, but larger cooling system itself requires more power to drive the fans and pumps, increasing the power load, which necessitates more cooling.

4.2.1 Physical model

To properly simulate the performance of a fuel cell scooter, a computer model was created based on the physical properties of the scooter. This model calculates the instantaneous power required from a scooter's engine as it travels through various driving patterns, and derives various numerical performance characteristics: fuel consumed per kilometer of travel, maximum power during the driving cycle, average power during the driving cycle, amount of energy recovered in regenerative braking, and overall hydrogen-to-mechanical-work conversion efficiency.

For the MATLAB program listing, please see Appendix F.

This power is calculated as the dot product of the current velocity of the vehicle and the various forces acting upon it, divided by the motor and controller efficiency, plus the auxiliary power demanded by various lighting and control systems, plus "parasitic" power required by the fuel cell blowers and coolant pumps. The road is assumed to be level. There are several different physical

forces to consider: air resistance (drag); the rolling resistance of the wheels; the force of gravity, which is not necessarily perpendicular to the velocity if the vehicle is traveling uphill or downhill; and the normal force of the ground acting upon the vehicle. These forces must sum to zero if the vehicle is to be held at a constant velocity, or to a net forward acceleration times mass if the vehicle is to accelerate.

Figure 4.1 Free-body diagram of scooter

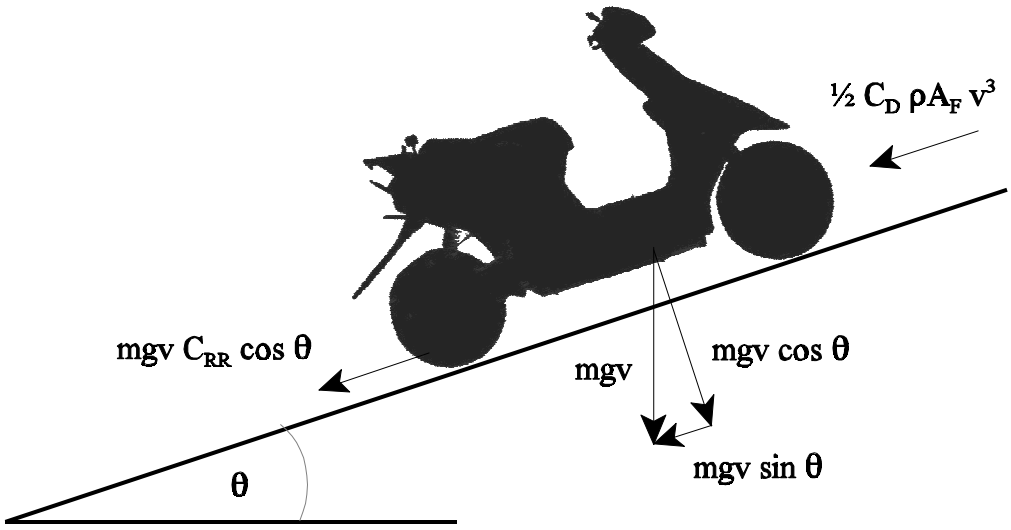

In the computer model used to simulate vehicle performance, the various power demands are summed to a total mechanical power P_{wheels} demanded "at the wheels" by the motion of the vehicle.

$$P_{wheels} = (ma v) +(mgv\sin\theta) + (mgvC_{RR} \cos\theta) + (½ \rho_{air} C_D A_F v^3)$$

The variables are listed below.

m = total mass of vehicle, passengers and cargo

θ = angle of slope

a = acceleration of vehicle

v = velocity of vehicle

C_{RR} = coefficient of tire rolling resistance.

ρ_{air} = density of air, approximately 1.23 kg•m^{-3}

C_D = drag coefficient

A_F = frontal area

The terms are described one at a time:

Acceleration term. If the acceleration is negative - that is, the vehicle is decelerating - the first term can be negative. If the overall expression for P_{wheels} is still positive even though the first term is negative, it means that energy must still be supplied by the power source to the wheels to maintain the desired deceleration rate, because the drag and rolling resistances are so large. If P_{wheels} is negative, then the motor can be driven as a generator to regenerate some of the energy expended. A battery capable of reabsorbing this energy is needed, and less than 70% of the kinetic energy is recoverable. This figure is reduced if rapid deceleration is required, because the battery can only charge up at a certain maximum rate.

Slope term. The second term is the force of gravity resolved opposite to the direction of motion.

Rolling resistance term. The coefficient of rolling resistance is a function of tire pressure and deformation, and is the ratio of rolling resistance force to the load on the tires; it is fairly constant for a given tire.[9] A perfectly rigid wheel on a rigid, flat surface would have no rolling resistance,

but minor deformations in the wheel and properties of the road cause deviation from ideal geometry and thus irreversible losses.

Aerodynamic drag term. The drag coefficient C_D is a dimensionless constant that attempts to capture, in one term, an object's resistance to flow. C_D can vary from as high as 1.2 for a bicycle with erect rider to 0.47 for a sphere to 0.20 for a very aerodynamically-styled modern automobile.[10] Although the equation used to determine the drag power is a simplification, it avoids complex air flow simulation while preserving the general behaviour of the drag force with respect to velocity. The frontal area used here was measured for the scooter by projecting a bright light parallel to the front of the scooter and then measuring the area of the shadow on a wall behind.[11] Typical values are listed in Table 4.3.

The inefficiencies in the system are applied afterwards to determine how much power must be put out by the power source:

$$P_{output} = (P_{wheels})/\eta_{drivetrain} + P_{auxiliary} + P_{parasitics}$$

$P_{auxiliary}$ = power needed by auxiliary systems - headlights, signal lights, dashboard, etc.

$\eta_{drivetrain}$ = efficiency of the electric motor and controller subsystem - 77%

$P_{parasitics}$ = parasitic power needed by fuel cell system - blowers, fans, etc.

The parasitic and auxiliary powers are electric power requirements so they do not go through the 77% efficiency loss. A more sophisticated model would not use a single value of $\eta_{drivetrain}$ but rather employ an efficiency map to determine electric motor efficiency as a function of wheel speed and torque.

Factors not accounted for in this model include: turning, where the velocity is not parallel to the acceleration / deceleration direction; wind blowing at an angle to the direction of motion; resistances in other parts of the scooter. Friction in the transmission and similar losses are assumed to be captured by the drivetrain efficiency of 77% above, discussed in section 2.1.4.

4.2.2 Modeling parameter selection

Vehicle modeling parameters for a typical scooter are listed below with data for other vehicles for comparison. Although most two-stroke scooters weigh about 80 kg, the presence of lead-acid batteries and/or fuel cell plus hydrogen storage brings the mass of an electric scooter up to approximately 130 kg as in the case of the Honda CUV-ES with NiCd batteries.

Table 4.3. Typical modeling parameters

Vehicle	C_{RR}	C_D	A_F (m^2)	curb weight (kg)	auxiliary power (W)
Electric Scooter	0.014	0.9	0.6	130	60
Roadster Bicycle	0.008	1.2	0.5	10	0
Motorcycle	unknown	0.6	0.8	300	unknown
Ford AIV Sable	0.0092	0.33	2.13	1291	500
PNGV Automobile	0.007	0.20	2.0	920	400

The PNGV Automobile properties are targets set out by the Partnership for a New Generation of Vehicles,[12] except for the rolling resistance and auxiliary power which were obtained from separate studies.[13,14] The Ford AIV Sable is a light weight "aluminum intensive vehicle", a modern mid-sized sedan.[15] Motorcycle data was obtained for some of the parameters.[16] Finally, the bicycle data is for a"roadster" upright model.[10]

The scooter coefficient of tire rolling resistance was estimated to be 0.014, based on measurements done at the Desert Research Institute[17], while the drag coefficient and frontal area were obtained

from researchers at the ITRI Mechanical Industry Research Laboratory.[18] A slight mass dependence (less than 6%) in the drag coefficient reported by the MIRL researchers was ignored, and the largest measurement taken; the velocity dependence of the rolling resistance coefficient was likewise neglected. Note also that in scooters and bicycles the product of drag coefficient and frontal area can vary dramatically, depending on how the driver sits on the scooter. The values chosen were assumed to be for the rider in a typical position.

The curb weight was set at 130 kg, which was 30 kg more than the ZES-2000 but equal to that of the CUV-ES electric scooter. This choice was made to ensure that performance requirements would be met even if the lower ZES-2000 weight could not be reached, whether due to the extra structural weight needed to support the heavier power system, or due to the weight of the components themselves. The driver weight is defined as 75 kg.

Auxiliary power: in a typical scooter, the head lights, tail lights, and dashboard total about 50 W; assuming that these lights are always on, and that the 26.4 W turn lights are on 30% of the time, yields an average load estimate of 60 W.[19]

4.2.3 Relative importance of various factors

Now that the parameters are defined, power requirements are calculated for (i) a scooter traveling at constant velocity at various slopes, and (ii) a scooter traveling with constant velocity at various speeds, and finally (iii) power required for various accelerations starting from 30 km/h. The total power shown below is the electric output from the power source including auxiliary power, but not subsystem parasitic loads (blowers, pumps, etc.) which are calculated later.

Figure 4.2. Cruising power required at various speeds.

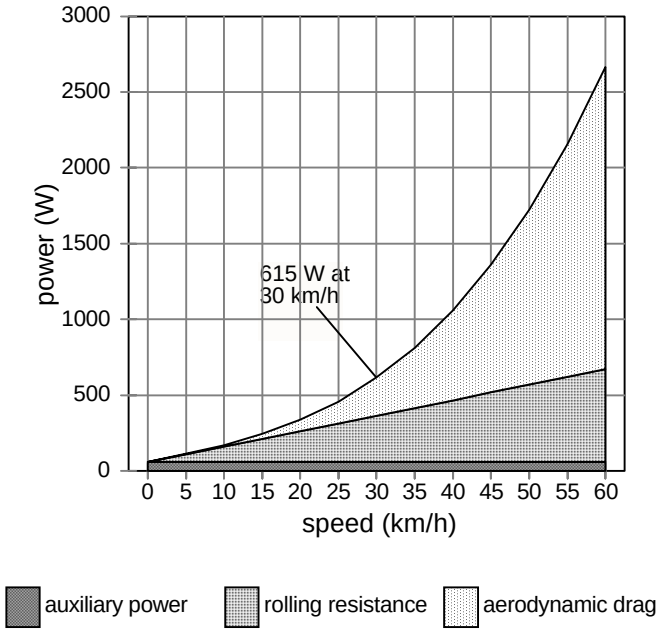

Figure 4.3. Power required to climb various slopes at 15 km/h

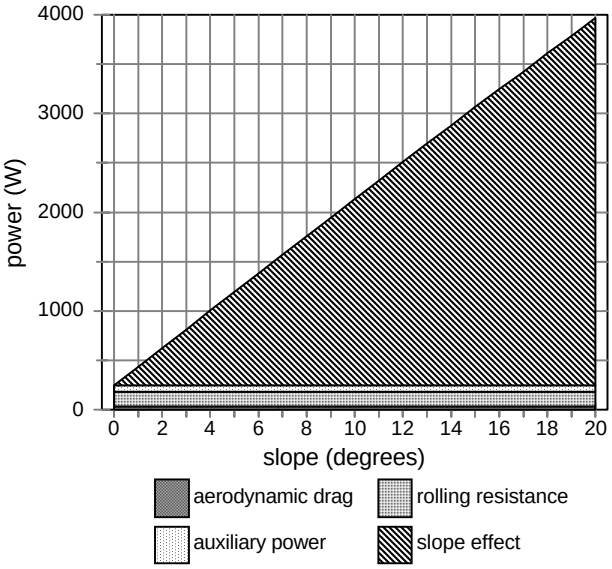

Figure 4.4 Power required for various accelerations from 30 km/h

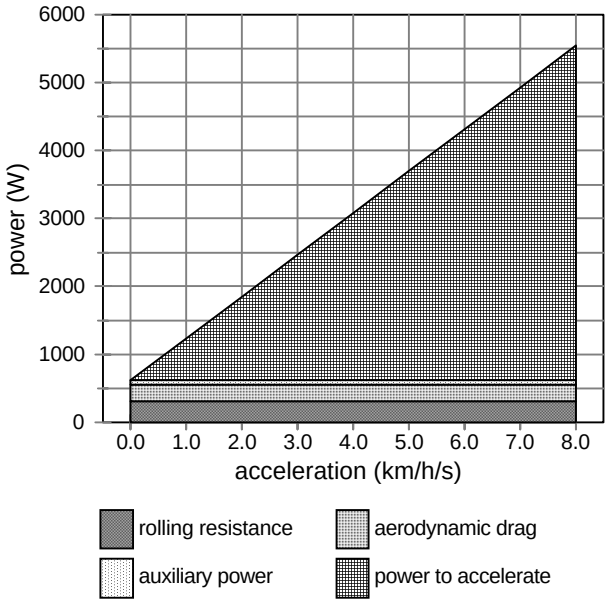

According to the model, continuous hill climbing as set out in the requirements (10 km/h at 15°, 18 km/h at 12°) require 2050 W and 3020 W out of the electric power source, respectively. Cruising at 30 km/h requires 615 W.

Due to the low speeds scooters are typically operated at, and the relative insignificance of the tire rolling resistance, the power needed for acceleration dominates the *maximum* power need. The effect of gravity on scooters traveling up a slope is also significant. In other words, for a scooter traveling on a level road and accelerating and decelerating in a typical stop-and-start urban driving cycle, the dominant term is *mav*, and the total power requirement is thus dominated by the mass of the scooter and the velocity/acceleration profile. Aerodynamic drag, which is not proportional to mass, tends to be a minor factor at the low speeds most scooters are driven at, especially in urbanized areas.

4.2.4 Validation

Some comparisons with others' results were provided to check the physical model. As in Figures 4.2 to 4.4, these results are for P_{output} *without* parasitic power, although they do include auxiliary power load and drivetrain efficiencies.

Table 4.4 Validation of physical model

	ITRI ZES-2000	DRI Sun Com	T. C. Pong requirements	This physical model
0 to 30 m in five seconds				2800 W
Maximum power (sustained for 5 seconds)	3800 W		3600 W	
Climbing a 15° hill at 10 km/h				2050 W
Climbing a 12° hill at 18 km/h	2160 W		2700 W	3020 W
Cruising at 50 km/h (sustained for 30 minutes)	1870 W		1800 W	1720 W
Cruising at 35.0 km/h		1200 W		810 W
Cruising at 30 km/h (sustained for 2 hours)	500 W		600 W	615 W
Cruising at 26.0 km/h		550 W		490 W
Cruising at 15.5 km/h		275 W		250 W
Cruising at 10.3 km/h		225 W		175 W

T. C. Pong, an electric scooter designer, listed a set of electric scooter power requirements for a 48 V motor system[20], while another set of data was measured from road tests of a Sun Com scooter by Arne LaVen of the Desert Research Institute.[21] The ITRI ZES-2000 results were from published papers.[22,2]

The physical properties of the other scooters were unknown but likely not more than 20% different from the drag coefficient, rolling resistance, and frontal area used in this study. A 77% drivetrain

efficiency was assumed for the ZES-2000, since these data were based on motor output; the other data points were from battery output measurements, and thus no drivetrain efficiency had to be assumed. The tabulated results are presented graphically below.

Figure 4.5 Validation of physical model

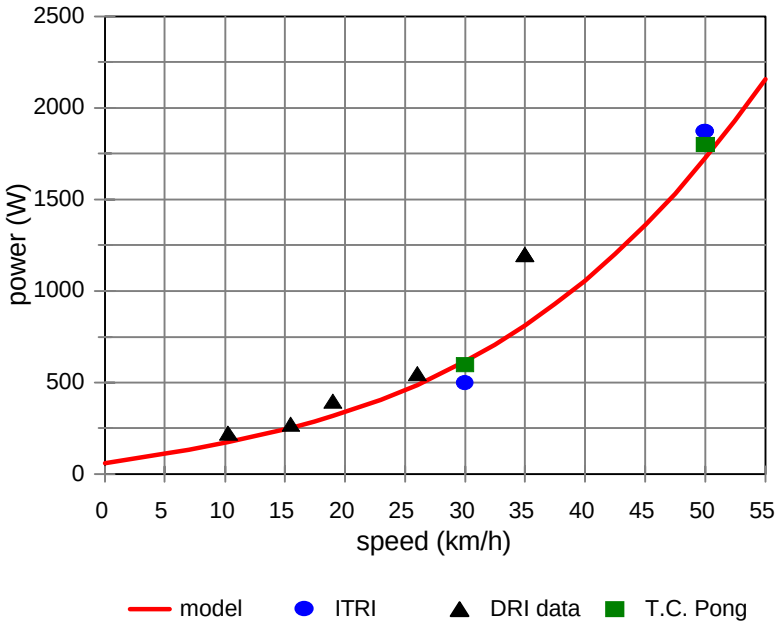

To verify the model in a different way, the cruising power of 615 W for 30 km/h was used to calculate average thermal efficiency if the drivetrain efficiency was also 77% for a mechanical system, and net fuel economy was 100 mpge as reported by various manufacturers. This means an average 9.5% thermal efficiency, a reasonable estimate for small two-stroke engines (As an example, a 34 cc engine designed for a blower, hedge trimmer, or chain saw has a peak thermal efficiency of 13.6%, or 20.6% for a prototype advanced stratified lean-burn design.[23])

If a 50% fuel cell conversion efficiency is assumed and parasitic losses are not included yet, then the equivalent fuel economy is 560 mpge; detailed analysis later will provide a more accurate result.

4.3 Driving Cycle

The main purpose of driving cycles, in the past, was to provide a schedule to put cars through to collect tailpipe emissions and, in the United States, to compute mileages for CAFE (Corporate Average Fuel Economy). Simulated driving patterns have high-power peaks that produce more emissions than a constant driving speed, and are more representative of actual driving behaviour. The typical procedure is to place the vehicle on a wheeled dynamometer and then to execute the driving cycle. Emissions are collected in a sampling bag and diluted with a predefined amount of air to obtain vehicle emissions in terms of grams per kilometer.

Typical automobile test cycles include the American FUDS (Federal Urban Driving Schedule), FHDS (Federal Highway Driving Schedule), and FTP (Federal Test Procedure 1975). American motorcycles are tested using a modified version of FTP ("mFTP"), with one part scaled down for motorcycle with engines less than 170 cc, so that the maximum speed is reduced from 91 km/h to 59 km/hr. Another method for testing motorcycles is the ECE-40 (Economic Commission for Europe) test procedure, which employs a much simpler and more abstracted driving cycle. Low acceleration rates and lack of transients mean that pollution is generally underestimated.

Figure 4.6 mFTP: modified Federal Test Procedure

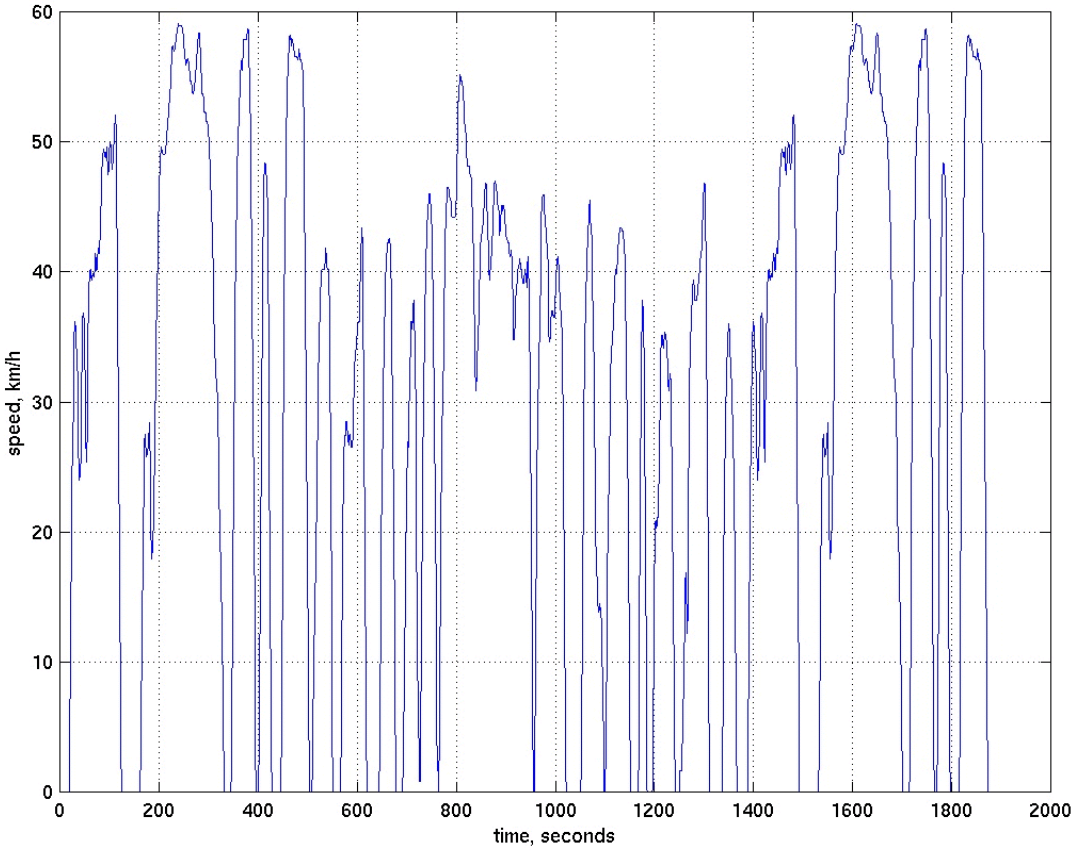

Figure 4.7 ECE-40

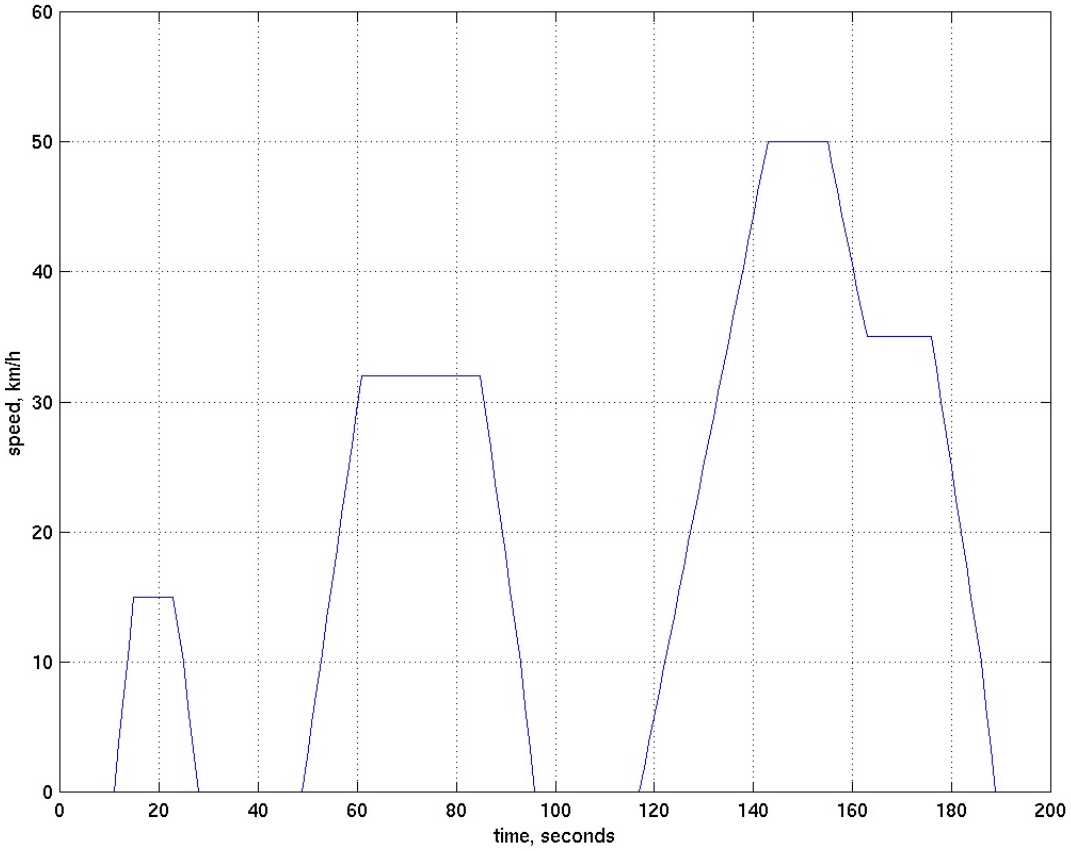

In recent years, driving cycles have been paired with computer models of road load, as described above, to predict and model vehicle performance.

4.3.1 TMDC

Driving patterns in Asian cities are significantly different from American highway driving, and even American city driving. For example, Taipei's congestion and frequent stops mean that average driving speed is less than 15 km•h^{-1}, and driving speed exceeds 40 km•h^{-1} only 10% of the time.[24]

The driving cycle used here, therefore, should be specifically targeted for the Asian driver. One

candidate is the Taipei Motorcycle Driving Cycle (TMDC), developed by researchers at the Institute of Traffic and Transportation at Taiwan's National Chiao Tong University. The TMDC is an actual velocity trace obtained by researchers who followed target vehicles on an instrumented "chase vehicle". The driving cycle consists of 950 velocity measurements (one per second) and each velocity measurement is rounded to the near $km \bullet h^{-1}$. An acceleration profile was derived by taking finite differences in temporally-adjacent velocity measurements.

Figure 4.8 Taipei Motorcycle Driving Cycle (TMDC)

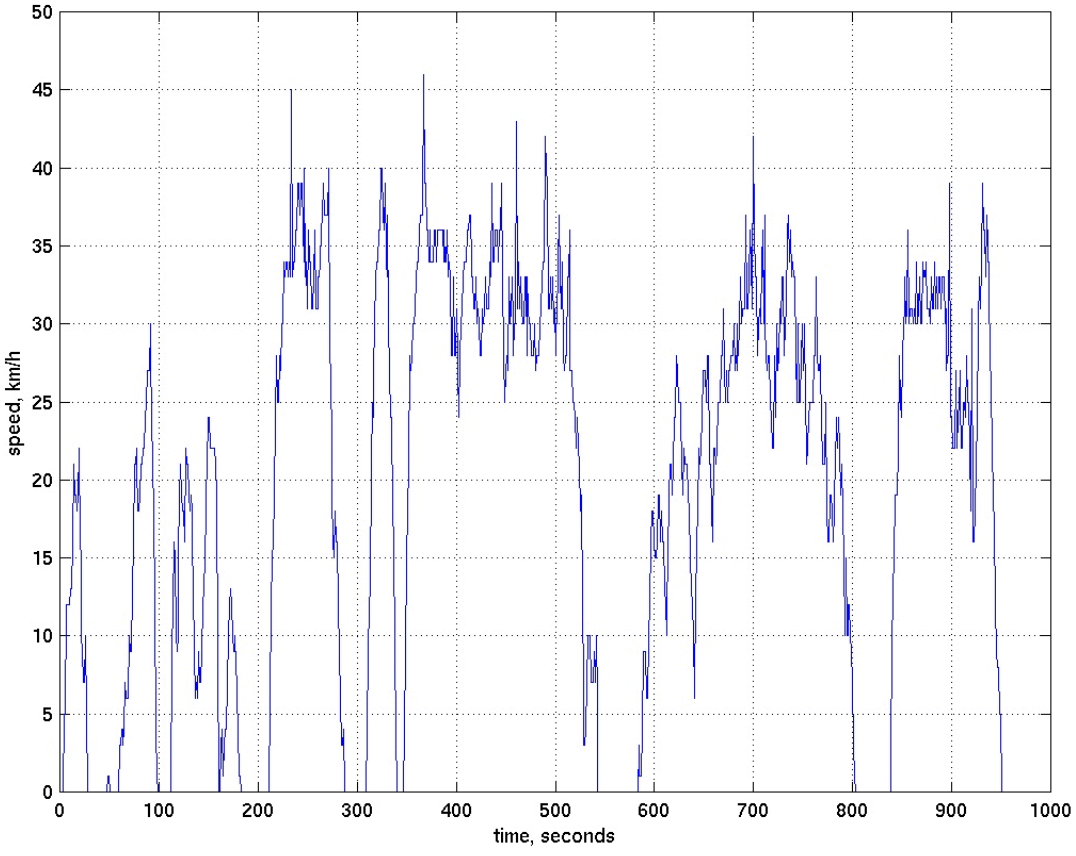

As a comparison of several characterizing parameters shows, the TMDC is different from FUDS and the motorcycle-modified FTP:

Table 4.5 Driving Cycle Comparison

	TMDC	modified FTP	FUDS
Total time	950 s	1873 s	1372 s
Total distance traveled	5109 m	15537 m	7450 m
Average speed	19.3 km/h	29.9 km/h	19.6 km/h
Maximum speed	46 km/h	59 km/h	57 km/h
Maximum acceleration	13.0 km/h/s	5.4 km/h/s	3.6 km/h/s
Maximum deceleration	-15.0 km/h/s	-5.4 km/h/s	-3.3 km/h/s
Fraction of time spent accelerating	31.5%	42.7%	39.7%
Fraction of time spent decelerating	30.3%	56.3%	34.6%
Fraction of time at steady non-zero speed	18.5%	1.0%	6.6%
Fraction of time at standstill (v = 0)	19.7%	15.2%	19.0%

The TMDC exhibits especially severe accelerations and decelerations - maximums of +13.0 km/h/s and -15.0 km/h/s, respectively. The maximum acceleration in the modified FTP cycle often used for testing vehicle emissions is 5.4 km/h/s, but the maximum acceleration observed in Bangkok motorcycle traffic is quoted as being 12 km/h/s.[25] (It is not clear what size of motorcycle the Bangkok number refers to). While it is true that scooters in Taiwan are driven in a more aggressive way than cars in American cities, these accelerations and their consequent power requirement of over 12 kW at the wheels significantly exceed the maximum performance capabilities of scooters 125 cc or less.

One important ramification of the high accelerations and decelerations is that a significant amount

of energy can theoretically be recovered by regenerative braking. Also, maximum power is much larger than average power.

Note also in Figure 4.8 “jitter” in the velocity reading. Errors due to rounding of the speedometer reading to the nearest km/h when the data was recorded create exaggerated accelerations and decelerations that did not reflect reality. For example, a speed that varied from 20.4 to 20.6 and back to 20.4 in two seconds would appear in the data as a one-second acceleration from 20 to 21 and back to 20. This jitter was analyzed below using the scooter model described previously. (The jitter starts from the base speed and oscillates up and down by 1 km/h)

Table 4.6 Effects of “jitter”

initial speed (km/h)	average power to accelerate 1 km/h faster in 1 second, then return to original speed (W)	power if speed was a constant 0.5 km/h faster (W)	jitter increases power by this fraction
5	179	117	53%
10	290	177	64%
15	416	252	65%
20	564	348	62%
25	740	472	57%
30	951	632	50%
35	1204	834	44%
40	1507	1085	39%
45	1866	1393	34%

The test shows that these oscillations produce significant variations in power required by the model that are not representative of actual driving.

4.3.2 Modification of TMDC

The TMDC is more representative of Taipei driving conditions than FTP or FUDS, but it has flaws that should be compensated for. As given, to achieve the performance of the TMDC simulation, a total power output of more than 12 kW is needed, significantly greater than the maximum power achieved by the internal combustion engines of even 125 cc scooters.

As a first attempt at improving the TMDC, the maximum speed was clipped to 40 km/h to more closely approximate reality. Accelerations were calculated from this less strenuous driving cycle; fortunately, these peaks were very brief and the integral under these parts of the velocity curve was small, so that there was very little difference in parameters of the driving cycle like total distance and fuel consumption. However, this first cut reduced maximum power only to 9.7 kW, so this technique was discarded.

Smoothing with a moving three-second box, as suggested by the researcher who developed the TMDC, was not adequate in attenuating the maximum peaks.

Another method of adjusting the driving cycle to reflect a more realistic assumption was to use a low-pass filter to get rid of the quantization jitter and to attenuate the very quick accelerations. Changing the characteristics of the low-pass filter would modify the final modeling results, so to choose an appropriate filter function, the results of the adjusted cycle were compared against reported data on scooter performance levels. (For example, the ZES-2000 was specified as being able to travel 30 m from a standstill in 4.5 seconds at maximum acceleration[1, 7], and the power required to achieve this acceleration was found to be 3.7 kW using the physical model. Similarly, a standard gasoline-powered scooter was quoted elsewhere as having a maximum power of 5.0 kW [2].

A maximum net electrical output power of about 5.0 kW seemed reasonable given these examples.)

The low pass filter was created as a transfer function defined to have a DC gain of 1 to not change the average value of the function acted upon (in this case the velocity as a function of time).

$$H(s) = \frac{1}{1 + \frac{2\pi s}{\tau_o}}$$

τ_o is the characteristic time, so that larger values of τ_o produce greater smoothing. This function was convolved with the velocity profile of the driving cycle to reduce high-frequency jitters and to attenuate accelerations and decelerations. The smoothing effect can be thought of as a multiplication (in the frequency domain) of the transfer function and the frequency spectrum of the driving cycle; due to the hyperbolic shape of the transfer functions, high-frequency components are attenuated while low-frequency components are increased.

The results of running the simulated scooter under the TMDC for various manipulations of the TMDC are presented below. The scooter parameters given in Table 4.3 were used. The FTP was compared to the smoothed driving cycles as a check to see if the results were close. The italicized choice was the one eventually selected.

Table 4.7 Results of different algorithms applied to TMDC; comparison to FTP

	original	**clip at 40 km/h**	**1/(s+4) smooth**	***1/(s+1.5) smooth***	**1/(s+1) smooth**	**mod. FTP**
average speed over cycle (km/h)	19.3	19.3	19.3	*19.3*	19.3	29.9
max net power from engine (includes drivetrain)	12.6 kW	9.8 kW	9.0 kW	*5.6 kW*	4.2 kW	5.5 kW
avg power from engine (no parasitics; includes drivetrain)	935 W	759 W	651 W	*566 W*	537 W	1254 W
max acceleration (km/h)	13.0	13.0	9.8	*6.4*	5.1	5.4
max deceleration (km/h)	-15.0	-15.0	-9.2	*-8.6*	-7.7	-5.4
std. dev of accelerations	0.79	0.76	0.61	*0.48*	0.44	0.58
avg. acceleration power (avg. of positive and negative)	63 W	59 W	38 W	*24 W*	20 W	34 W
avg. acceleration power (positive only)	370 W	355 W	285 W	*215 W*	188 W	289 W
avg. rolling resistance power	151 W	151 W	151W	*151 W*	151 W	234 W
avg. aerodynamic drag power	118 W	117 W	117 W	*117 W*	116 W	425 W
accel. power (when in motion)	1178 W	1129 W	678 W	*517 W*	446 W	674 W
rolling power (when in motion)	189 W	188 W	184 W	*179 W*	175 W	272 W
aerodynamic drag (when in motion)	147 W	146 W	143 W	*138 W*	134 W	495 W

Note that the average acceleration powers are very low because acceleration can be negative; the average acceleration power for positive results only is more indicative of how the energy is split between the various components. It should be noted, however, that negative acceleration power can be used to "cancel out" power demands from aerodynamic drag and rolling resistance. That is, when the vehicle is decelerating, the drag power and rolling resistance can be allowed to slow down the vehicle so negative accelerations are not entirely meaningless to the power calculation.

The mFTP results show much higher average power than the selected smoothed curve, due to rolling resistance and aerodynamic drag, which in turn are due to the average speed being 50% higher than the TMDC. On the other hand, the maximum power is very close to that of the smoothed curve, suggesting that a scooter designed for the TMDC will be capable of sustaining the FTP driving cycle which was originally designed for the more powerful motorcycles. The maximum mFTP power of only 5.5 kW is a telling indicator that the TMDC (unsmoothed) is too severe.

Smoothing dramatically decreases maximum accelerations and decelerations, and changes the acceleration characteristics of the driving cycle, but does not significantly change the other components; this is because acceleration is such a large component of maximum power but not such a strong determinant of average power.

The low-pass filter with a 3.1 second smoothing interval (italicized in Table 4.7) was chosen to smooth out jitter and reduce the maximum power required to on the order of 6 kW - specifically, 5.6 kW including auxiliaries but not including parasitics because parasitics are dependent on later calculations based on these results. This is comparable to modern 50 cc scooters, with maximum power closer to those of the mFTP.

Figure 4.9 Smoothed TMDC

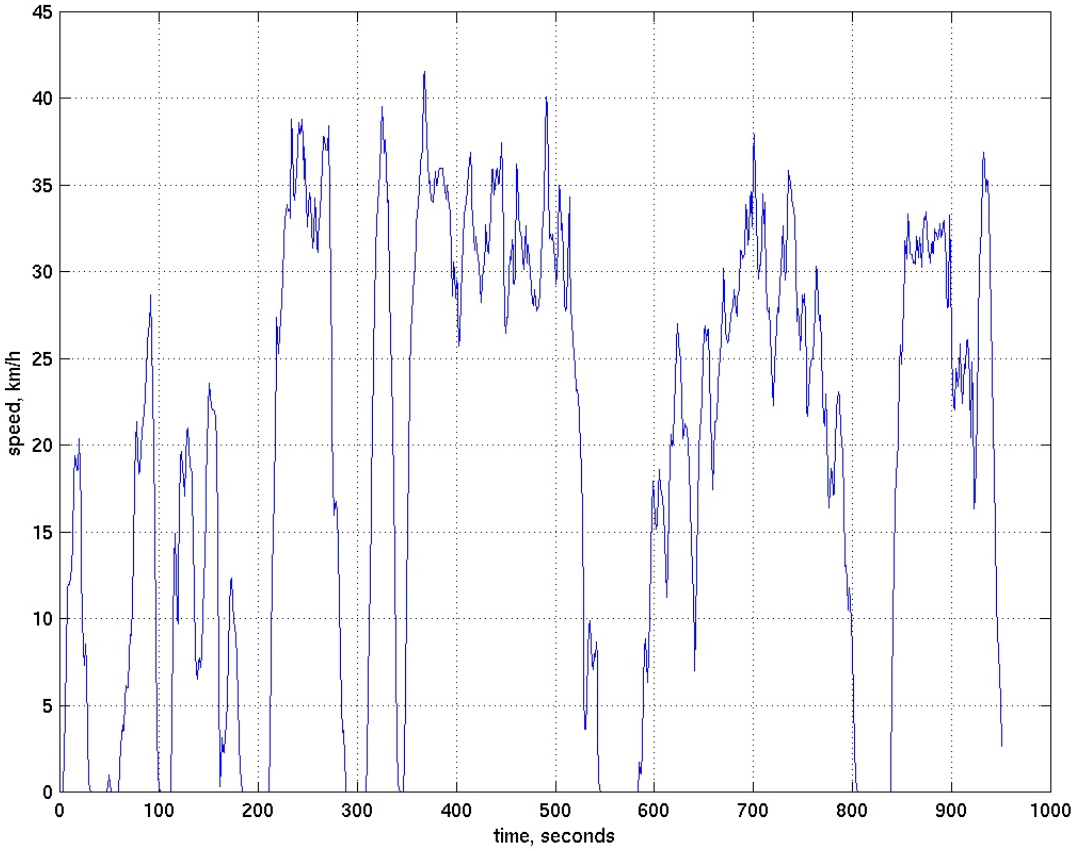

The "smoothed TMDC" driving cycle was used for all further calculations, and referred to as simply the TMDC. Note that the energy finally dissipated in braking (i.e. where deceleration "power" is greater than aerodynamic drag and rolling resistance powers) is 116 kJ over the 950 second cycle, or 122 W in the smoothed TMDC. This is about 20% of the 566 W engine output.

4.3.3 Torque vs. rpm requirements

Looking only at the maximum power produced by the electric motor and the maximum power produced from the fuel cell or battery is not sufficient to ensure that the power demands of everyday driving are met. This is because the total output is limited by the maximum power of the motor, but

also by other factors like the maximum current (which sets a maximum torque even when the speed might be low).

Torques are summed about the axle of the drive wheel; the rolling resistance and acceleration "torque" have moment arms equal to the radius of the wheel (15.8 cm), while the drag force is assumed to be act at the center of mass of the scooter, 20 cm above the axle. In order to ensure that the required torques could be produced, the model results were illustrated as a scatterplot of torque versus speed. Imposed on this graph was the maximum performance curves of the chosen Unique Mobility (UQM) brushless DC scooter motor rated at a nominal 3.6 kW.

Figure 4.10 Torque vs. rpm during TMDC

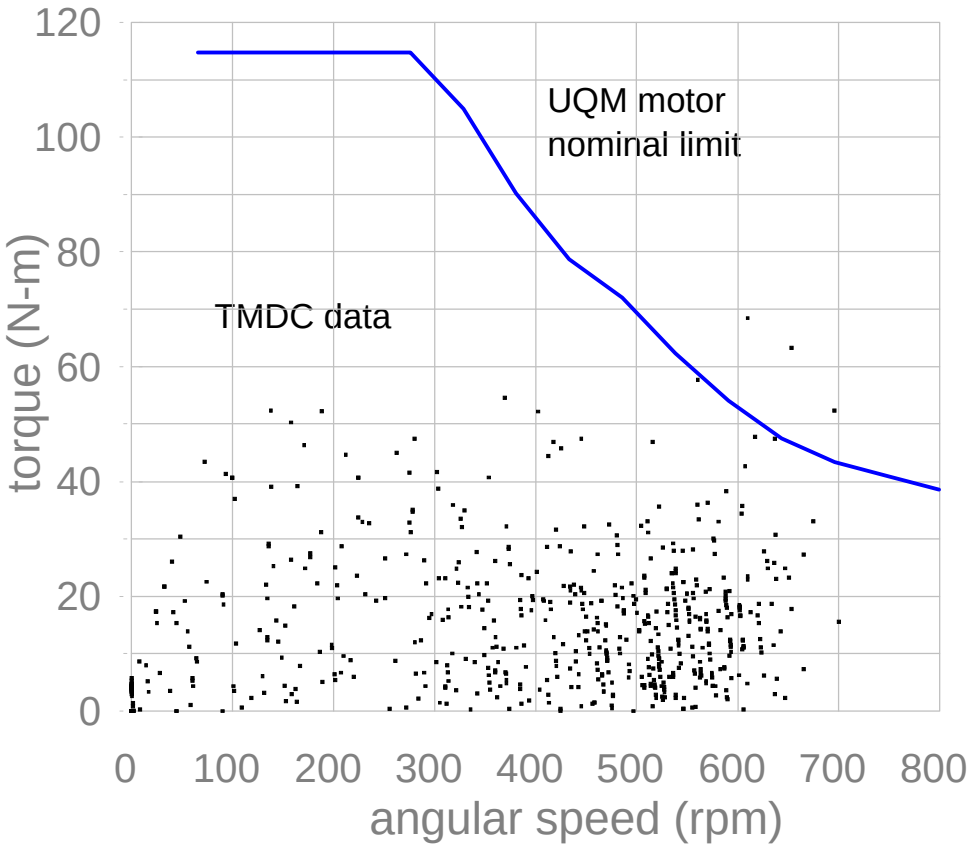

Note that at three one-second time intervals, torque required exceeds that available from the UQM motor. These peaks represent the maximum power of 5.6 kW of electrical output, which translates to 4.3 kW of mechanical power after the 77% drivetrain efficiency - greater than the 3.6 kW maximum output of the UQM motor. The assumption was made that the three outliers were sustainable for short periods of time.

4.3.4 Modeling results

The results of the TMDC driving cycle are shown below.

Figure 4.11 Power required in TMDC

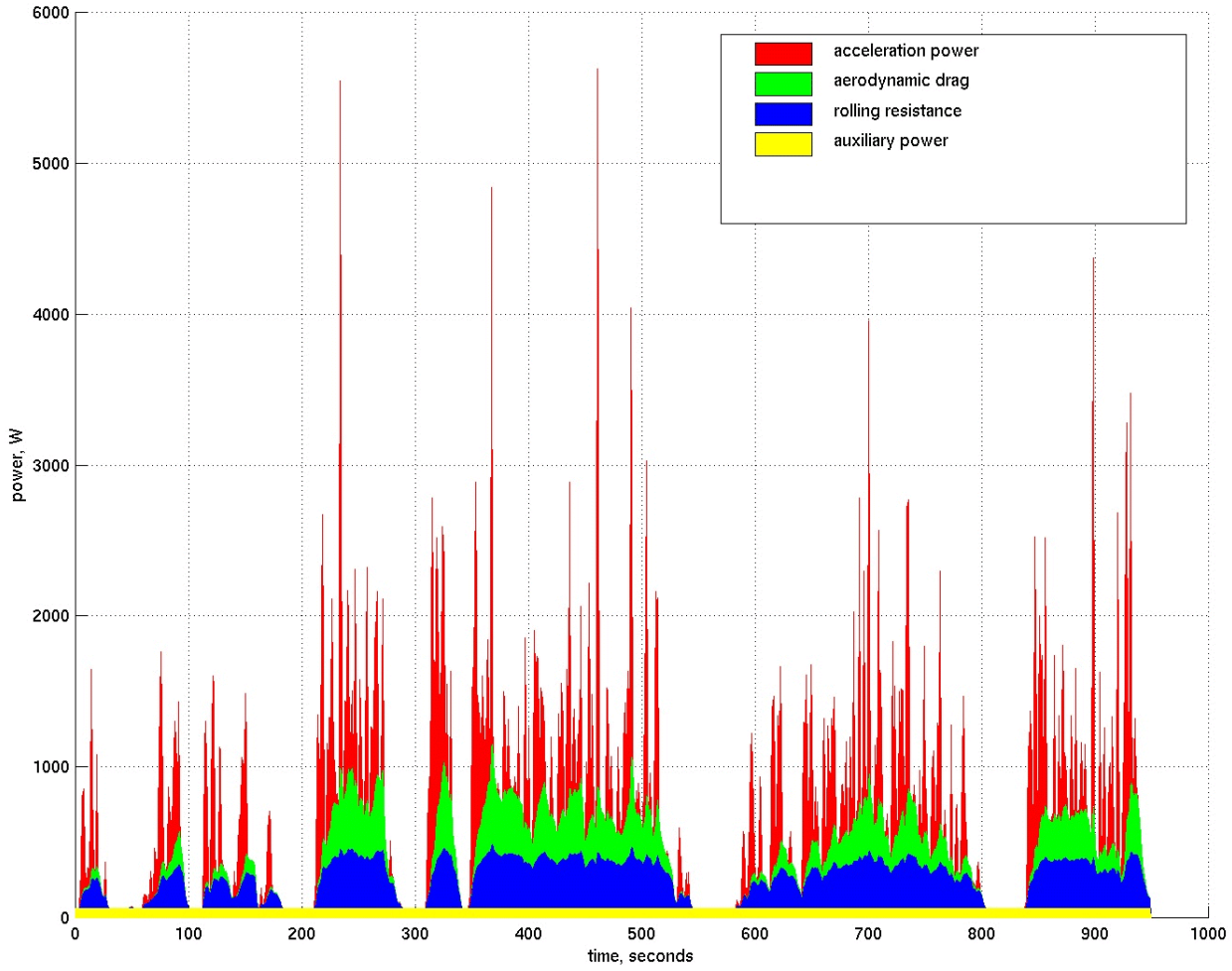

Acceleration power demands the greatest peaks in the cycle, and also accounts for most of the energy in the cycle (not including braking energy recovered from negative accelerations). Rolling resistance accounts for somewhat less energy, and aerodynamic drag even less. The 60 W of auxiliary power is at most 10% of the average power.

Interestingly, the average power is approximately one tenth of the maximum power. The extreme variability in the power demands suggests that hybridization would be useful, with a battery providing surges of extra power during bursts of acceleration and also the capability to store braking energy.

The physical model shows that the power needed, under the TMDC, is an average 566 W of electric power out of the fuel cell without parasitics. A complete analysis of fuel economy, however, requires a polarization curve of efficiency versus net power, and an understanding of the parasitic power. This is in section 4.5.

4.3.4.1 Battery powered scooter

The parasitic power requirements of the fuel cell have not yet been calculated but there is enough information here to calculate performance of a scooter running on just a single battery. The power output is the same as the fuel cell power output except without the parasitic requirement. A total of 4.1 kWh (output) are needed to store enough electricity for 200 km of range.

Table 4.8: Taiwan battery-powered scooter performance

	TMDC driving cycle	**30 km/h cruising**
Average speed	19.3 km/h	30 km/h
Average power (electric output)	566 W	615 W
Mileage in terms of electric output	35.5 km per kWh-output	48.8 km per kWh-output
Maximum power output	5.6 kW	615 W
Total energy storage for 200 km at 30 km/h		4.1 kWh

The battery requirements, given the different USABC battery technology predictions and a 4.1 kWh storage capacity, are compared to today's lead-acid batteries.

Table 4.9: Various battery-powered designs for Taiwan scooter

	Lead-acid: today's battery	**Mid-Term advanced battery**	**Long-Term advanced battery**
Weight	117 kg	62 kg	25 kg
Volume	58 L	36 L	16 L
Cost	$245-$735 (current)	$735 (mid-term)	$490 (long-term)

For the lead-acid battery, the critical assumptions were 35 Wh/kg and 70 Wh/L. Note that in the mid-term and long-term cases, the battery weight and volume are determined by the maximum energy requirement, not the *power* requirement. In fact, a mid-term battery of this size would offer 7.7 kW of maximum power, while the long-term battery would output a maximum of 8.2 kW! The limiting factor in battery size and weight for these batteries is energy storage, not power storage. Section 4.7 on hybrid design shows how decoupling the energy and power functions of the battery improve the system.

Today's ZES-2000 scooter with far shorter range than the systems described above gives an idea of how much room is available in the scooter: at least 44 kg and 15 L (not including the electric motor and controller). The next step is to design a fuel cell power system within these size and weight parameters that can output a continuous 610 W for 30 km/h cruising for 200 km (or 6.7 hours); produce a 5.6 kW maximum output; and generate 3.2 kW of continuous hill climbing power.

4.4 Fuel Cell System Design and Integration

4.4.1 Design tradeoffs

The fuel cell stack is specified by only two independent variables plus the polarization curve and the maximum power:

1. Maximum power
2. The polarization curve
3. Power density
4. Number of cells in the stack

(Note that, instead of power density and number of cells, we could have equivalently chosen area per cell and total active area of all cells)

4.4.1.1 Maximum power and the polarization curve

A maximum gross fuel cell power of 5.9 kW is assumed from parasitic requirements calculated in section 4.4.5. This is slightly over the sum of the maximum TMDC requirement of 5.6 kW net power plus an initial estimate of 300 W for parasitic power losses. The parasitic requirements are discussed in greater detail later on, but for now it is enough to say that they are approximately linear with gross power output so that maximum parasitic power occurs at maximum gross power.

The polarization curves used are those derived from Energy Partners for single atmospheric-pressure *cells*; these are extrapolated to be equal to future *stack* performance.

Figure 4.12 Polarization curve

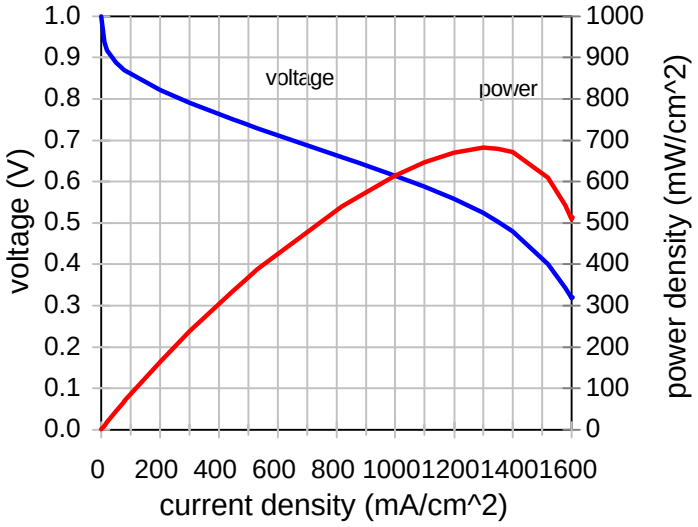

Data is from Barbir is for a single cell running on hydrogen/air, with a Gore MEA and operating temperature of 60°C. Air-side stoichiometry is 2.5.[26]

4.4.1.2 Power density

The first choice to make is to determine the power density to operate at, under conditions of maximum power. If maximum output is arranged to take place at low power density, the left portion of the polarization curve is used (since power density scales almost linearly with current density); voltage, and thus efficiency, are high in this portion of the curve. However, a large total active fuel cell area is needed and much electrolyte membrane and platinum will then be required. The stack size will be larger.

If a low total area is used, then power density per area is high. The power density curve peaks at high current densities, with correspondingly low voltages and low efficiencies. (The low total area can be achieved by a combination of low cell area and/or few cells). Total price is a monotonic function of total area, so the high power density approach results in a smaller stack and cheaper stack, although efficiency would suffer and consequently hydrogen storage requirements for a given range would be higher.

Power density also controls the flow rates of the air and hydrogen reactants. The flow rates are functions of the designed hydrogen utilization and oxygen stoichiometric ratio, and also of the efficiency of the fuel cell; low efficiency means that more reactants must be flowed for a given power output. Thus, for a given power level, high power densities mean higher flow rates because they operate in the low voltage (low efficiency) portion of the polarization curve. The sizes and costs of air management equipment are determined in part by flow rate, but it should be noted that the scooter application demands flow rates far below those normally available for vehicle systems so most systems for scooters based on automotive designs would be oversized anyway.

To maximize efficiency and produce a small, cheap fuel cell, a high power density is selected. According to the polarization curves presented, power is maximized at about 1300 mA•cm^{-2}; to be conservative and leave room for unusual bursts of speed, a point below this power peak is chosen: 1000 mA•cm^{-2}. At 1000 mA•cm^{-2}, voltage is 0.614 V, and power density is thus 614 mW•cm^{-2}. For 5.9 kW at this point, 9.6 x 10^{3} cm^{2} of active area are needed.

4.4.1.3 Number of cells

The number of cells is a function of the desired operating voltage. The electric scooter industry in Taiwan is standardizing on 48 V electric motors, so the number of cells is chosen so that the stack operates in the vicinity of 48 V at the most common power demand; note that in a fuel cell, as the total power output changes, the voltage varies as well.

The DC-to-DC conversion is assumed to be performed by the motor controller, and is included in the 77% drivetrain efficiency. (In comparison, standalone DC-to-DC converters from Vicor offer approximately 410 W/L and 381 W/kg, with efficiencies of 80%-90%; prices are on the order of 1 $/W.[27,28]) All parasitic power – fans, pumps, blowers, etc. – should be DC to avoid the large additional expense of a DC-to-AC inverter.

The average TMDC power demand is 566 W, and later modeling in shows that the final result including parasitic power (after iterative calculation) is 674 W. With a 9.6x10^{3} cm^{2} total membrane area, the power density is 70 mW•cm^{-2}. To obtain this power density on the polarization curve, 79 mA•cm^{-2} and 0.870 V are needed - only 8% of the maximum current density, and high up on the efficiency curve. The system is designed to run at 48 V at this point, and dividing 48 V by the 0.870 V per cell gives a minimum of 56 cells. Area per cell is then approximately 170 cm^{2}.

Table 4.10: Fuel cell design parameters at maximum power

	maximum power	hill climbing power	average TMDC power
Power with parasitic load	5.9 kW	3.2 kW	665 W
Current density	1000 mA•cm^{-2}	448 mA•cm^{-2}	79 mA•cm^{-2}
Stack current	172 A	76 A	13 A
Cell voltage	0.614 V	0.751 V	0.870 V
Power density	614 mW•cm^{-2}	336 mW•cm^{-2}	69 mW•cm^{-2}
Stack voltage	34.2 V	42.0 V	49.0 V
Open-circuit voltage (occurs at minimum power; parasitics not included)	56.0 V		
Total active area needed	9600 cm^2		
Total number of cells	56		
Active area per cell	170 cm^2		

(Note that this stack could also have been designed as two electrically parallel stacks of 56 cells each 85 cm^2 in area and with half the maximum current (86 A), or various other configurations).

4.4.1.4 Flow rate parameters

It is further assumed that the air flow rate is 2.5 times stoichiometric (to reproduce the performance of the Energy Partners polarization curve) and that the hydrogen consumption is 100% due to dead-ended operation. The surplus air lessens the effects of oxygen depletion in the cathode as oxygen is consumed by the fuel cells and also helps to push out product water. The exhaust gas flow rate was calculated by summing the input gas streams of air (21% oxygen) and hydrogen and then subtracting the hydrogen and oxygen consumed. The water is assumed to emerge as liquid so is not included in the exhaust flow rate. From this set of data, the following flow rate characteristics are

derived:

Table 4.11: Flow rate parameters at maximum power

	volumetric	molar	mass
hydrogen intake rate	2.6 CFM	0.05 mol•s^{-1}	0.1 g•s^{-1}
air intake rate	15.6 CFM	0.30 mol•s^{-1}	8.6 g•s^{-1}
total exhaust gas rate	16.9 CFM	0.27 mol•s^{-1}	7.8 g•s^{-1}
(liquid) water production rate	0.9 mL•s^{-1}	0.05 mol•s^{-1}	0.9 g•s^{-1}

4.4.2 Gas subsystem

As discussed previously, the pressure drop in fuel cell stacks has been estimated at 0.5 - 2 psi. With a 50% blower efficiency, worst-case 2 psi air drop, and the calculated 15.6 cfm of air flow, this is a maximum theoretical power consumption of 200 W. In theory, this scales down linearly with decreasing flow rate, but in practice the pressure drop also decreases as a function of flow rate so the decrease is somewhat sharper than linear. A heavy-duty blower that could be used to provide the required output is the Ametek 5.7" BLDC three-stage blower, model 116638-08. Its volume flow capacity is much higher than the 16 cfm required, but it is the smallest model capable of the relatively high 2 psi needed.[29] Retail cost is $430.

The blower power was modeled in the simulation as a linear 50-250 W load, for a gross power output of 50-5850 W. This is a conservative calculation based on comparison with a reported parasitic power draw of 105 W for a 24 VDC Ametek blower at 1.3 psi for a 4 kW nominal power fuel cell.[30]

On the hydrogen side, a pressure regulator expands the hydrogen from either the 1-10 atm partial

pressure of a metal hydride system, or a 3600 psi (260 atm) pressure of a compressed gas system.

4.4.3 Water subsystem

A low fuel cell operating temperature of 50°C is chosen to minimize evaporation losses and eliminate the need for external humidification (and complex control of that humidification). The maximum allowable fuel cell temperature is set to 65°C.

According to Mazda Demio documentation, external humidification requires an additional 15% in stack volume, but thin wicking polymer membranes can allow water to be backdiffused from the cathode to the anode to keep the membranes humidified without external humidification.[31] The wicking polymers could alternately transfer water from a reservoir to pre-humidify incoming air if humidification turns out to be necessary after all.

4.4.4 Cooling subsystem

There are several heat flows to consider in fuel cell systems.

1. Waste heat must be removed from the stack with a liquid coolant loop.
2. The liquid coolant must have heat removed at the cold side with a fan.
3. Air entering the system may be preheated in order to retain more water from any humidification
4. The humidification water, if any, can be preheated as well
5. Reformers, if present, require temperatures of at least 300°C to operate, and may produce net heat
6. Heat must be supplied to the metal hydride system, if one exists, in order to desorb the hydrogen.

To optimize the system, some of the flows can be combined. For example, the coolant loop is a convenient source of heat for a metal hydride storage system, while the blower could be designed to draw its input air from behind the coolant radiator.

All heat flows in the system are functions of the instantaneous power, since the waste heat, hydrogen demand, and air demand all scale according to the efficiency curve with respect to power in almost the same way. The maximum heating load occurs at maximum power in the driving cycle - at 5.9 kW of gross electric output, efficiency is 41.2% and heat output is 8.4 kW. However, the *average* heat load during typical TMDC driving is much lower, only 742 W. Given sufficient thermal mass, temperatures in the stack can be kept near the design point without the use of a large radiator. The ultimate concern is to keep the temperature low to avoid evaporating too much water from the membrane.

In comparison, a 20% efficient 5 kW internal combustion engine outputs 20 kW of waste heat. The difference is that this load is produced at high temperatures and thus is easily rejected to the environs by air blowing over cooling fins

There are two beneficial cooling effects that are not quantified here. First, fuel cell efficiency is calculated on a higher heating value basis, meaning that the product water is assumed to emerge solely as liquid water. In fact, some is vaporized and this removes heat from the system, making the cooling design somewhat conservative.[32]

Second, some heat is "used up" by the intake air. At a maximum flow rate of 8.6 g/s, an intake temperature of 30°C, and a heat capacity for air of approximately 1 $J \cdot g^{-1} \cdot K^{-1}$, 170 W of heat are required if the incoming air heats up to the stack temperature of 50°C. This small amount of cooling

is not included below but is noted for the sake of completeness.

4.4.4.1 Cooling from storage system

Here, cooling from metal hydride adsorption is discussed, along with more conventional cooling. The temperature of the fuel cell stack is modeled over the entire driving cycle to ensure that the fuel cell remains within its designed limits of 50°C and 65°C.

TiFe metal hydride systems consume 28 kJ of heat per mole of hydrogen desorbed. In the system, the maximum heat production is 8.4 kW and occurs at the maximum gross power of 5.9 kW. Here, hydrogen consumption is 0.05 moles•s^{-1}, so the hydride takes up 1.4 kW (16.7%) of the waste heat. This percentage increases as the fuel cell is turned down to lower powers, because the number of moles of hydrogen per heat output increases due to the greater efficiency; over the full range, the metal hydride system eliminates 16.7% - 30.2% of the waste heat. This reduces the size of the radiator and decreases the parasitic power required for cooling.

Figure 4.13 Metal hydride cooling vs. power

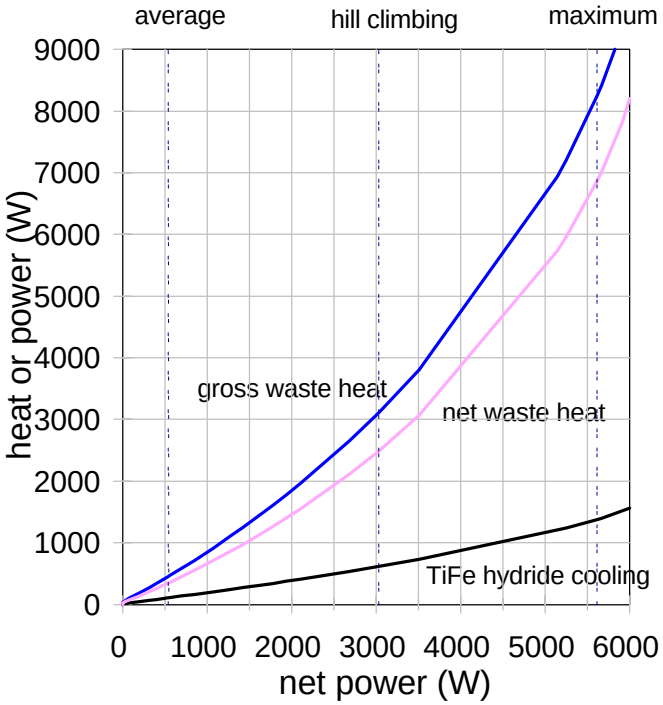

For this reason, metal hydrides have a significant advantage over gas cylinders. Combining a water cooling system for the fuel cell with the metal hydride allows the transfer of this heat, although a backup heating system might be necessary for startup heating and active control of the metal hydride temperature. This backup system could be a resistance heater wrapped around part of the metal hydride, connected to the startup battery. (The pressure of hydrogen gas over the hydride at room temperature would be greater than atmospheric, so there would be some hydrogen at startup. However, with waste heat slow to reach the hydride, an extra heater could provide a faster flow rate for immediate high power).

4.4.4.2. Active cooling

There are several possibilities for liquid cooling.

1. Cooling is provided by a closed loop water coolant circulated at constant flow rate through the stack by way of cooling plates. The hot water exiting the stack is circulated to a heat exchanger exposed to the atmosphere, where a fan enhances heat transfer. The fan speed can be increased to provide additional cooling. Alternately, a constant-speed fan can be used in a thermostat mode (allowed to switch on and off as needed), allowing the coolant temperature to fluctuate.

2. Variable coolant flow rate, fixed fan speed. As stack output power increases, the coolant circulation speed is increased. The change in temperature of coolant as a function of power is dependent on the heat exchanger properties. A variable-flow pump is needed.

3. Variable coolant flow rate, variable fan speed.

4. The pump is eliminated, reducing weight, cost, and parasitic power; instead, a refrigerant designed to boil at the fuel cell operating temperature is used in conjunction with a check valve, and the expanding gas drives circulation in the coolant loop.

In all cases, water circulation should be stopped altogether when the engine is warming up to operating temperature, so some kind of thermostat (if not variable) control should be employed for the coolant loop.

The heat exchanger cooling factor, in terms of watts of heat dissipated per degree of temperature

difference between the coolant and ambient temperature, provides an upper limit on how much heat can be removed from the stack at a constant output power. Charts of cooling factor (W/K) as a function of air flow rate and coolant water flow rate for various heat exchangers, in conjunction with charts of pressure drops, were used to determine parasitic loads for the radiator fan and coolant pump, respectively. This information was obtained from Lytron, a heat exchanger manufacturer (see Appendix C)

Continuous hill climbing determines maximum continuous power output (intermittent higher power output, like that of the TMDC, is interspersed with many periods of low power output). To satisfy the hill climbing requirement of 18 km/h at a 12° slope, 3200 W (gross output with parasitics) are required. Efficiency at this output point is 50.7%, waste heat is 3.1 kW and hydrogen consumption is 0.022 moles/s. The 28 kJ/mol of the hydrides eliminates 20% of the waste heat, leaving 2.5 kW, or 100 W/K that must be dissipated for a fuel cell at the design maximum of 65°C and a worst-case ambient temperature of 40°C (ΔT=25°C). An extra 10 W/K was added for a design specification of 110 W/K, which is met by an M14-120 radiator at a retail cost of $240.

Due to the lack of space at the front of the scooter, the radiator would likely have to be installed at the sides of the rear compartment, where flowing air would pass over the radiator pipes.

Here, the assumption is that the coolant pump and cooling fan draw power all the time. This is not a realistic assumption in that the power should be turned off when cooling is not needed (to ensure the fuel cell is above the minimum operating temperature). However, it is a safe assumption in that it overestimates (slightly) the power needed for parasitics, especially since pump and fan power draw needs are uncertain.

4.4.4.3. Heat generation under the TMDC

Maximum heat dissipation is determined by continuous hill climbing, but to ensure that the short spikes of high heat generation in the TMDC do not push the fuel cell temperature past 65°C, the temperature of the stack was simulated using a simple model. Heat generation under the TMDC simulation has the same general shape as the power output graph, but the peaks and valleys are exaggerated because efficiency decreases with increasing power output.

Figure 4.14 Heat generation as a function of time in TMDC

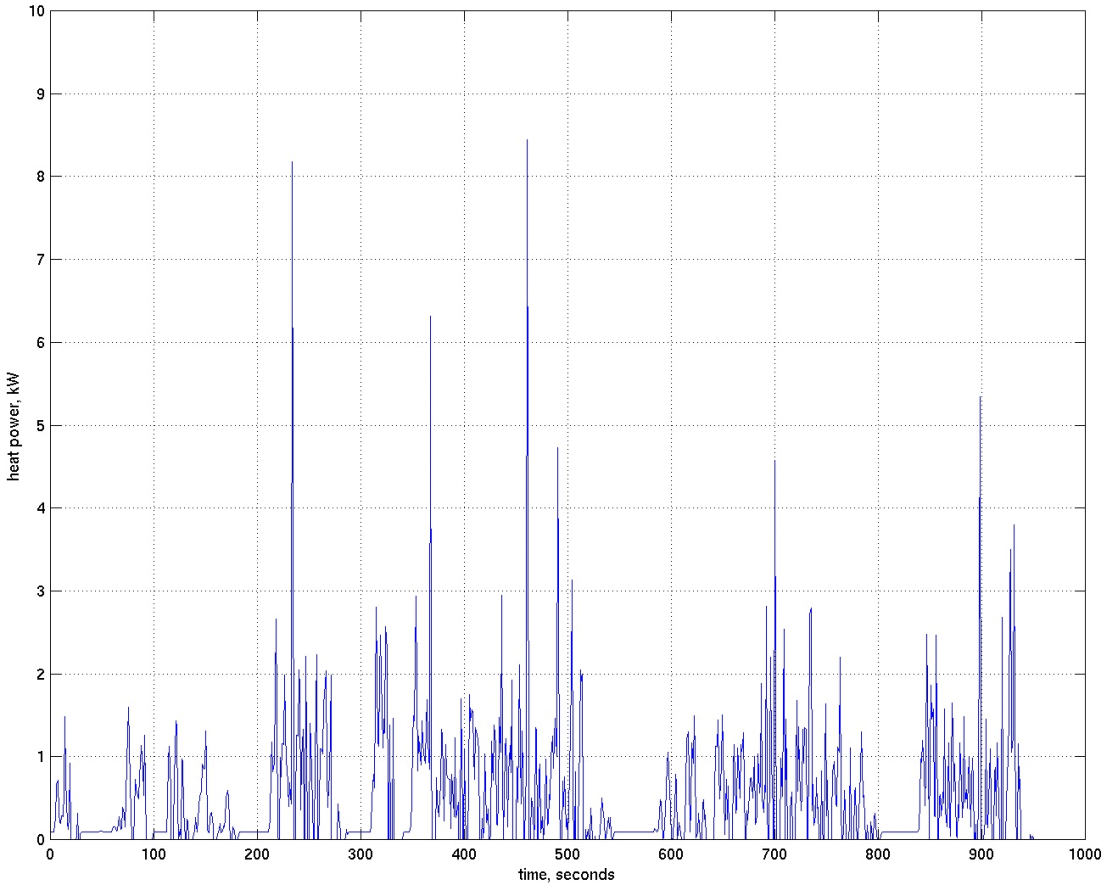

Note that average heat generated is 742 W for the 5.9 kW stack. After the metal hydride heat absorption is included, this decreases to an average load of only 393 W. The net heat generated was calculated for each step of the TMDC and used to calculate a change in temperature for the stack. The purpose of this further test was to make sure that the cooling factor (sized for continuous load) would be enough to keep stack temperature below the design limit of 65°C through the peaks and spikes of the TMDC.

The heat capacity equation used was

$$Q = M C \Delta T$$

for heat Q, stack mass M, average heat capacity T, and change in temperature ΔT. This was discretized for each time step, and the mass and heat capacity were separated into the different materials found in the stack, resulting in the following equation:

$$\frac{\Delta T}{\tau} = \frac{\dot{Q}}{M_1 C_1 + M_2 C_2}$$

$\dot{Q}$ is the heat power generated in a given time interval; M is the mass of the parts of the stack that make up the bulk of the total weight and are closest to the membranes (i.e. “1" for the stainless steel separator plates and “2" for the polypropylene gaskets); C is the heat capacity of the stack materials; and τ is the length of time of a single time step of the model.

Table 4.12 Stack temperature model parameters

parameter	value	note
Mass of 316 stainless steel separator plates	2.0 kg	0.5 $J \bullet g^{-1} \bullet {}^{\circ}C^{-1}$ specific heat capacity
Mass of polypropylene gaskets	0.8 kg	2 $J \bullet g^{-1} \bullet {}^{\circ}C^{-1}$ specific heat capacity
Heat capacity of stack as a unit	2.6 $kJ \bullet {}^{\circ}C^{-1}$	Weighted sum of steel and polypropylene
Specific heat capacity of stack	0.93 $J \bullet g^{-1} \bullet {}^{\circ}C^{-1}$	c.f. water at 4.2 $J \bullet g^{-1} \bullet K$
Heat exchanger cooling factor	150 $W \bullet K^{-1}$	maximum cooling
Ambient temperature	40°C	worst case
Heat removed by metal hydride	28 $kJ \bullet mol\ H_2^{-1}$	minimum 17% of waste heat

The assumption made was that most of the heat would be trapped inside the plastic housing (designed for electrical insulation), removed mainly by the active cooling system. The membrane itself is negligible because it is so light. This simple model does not include the effects of heat conductivity - just heat capacity.

The cooling system was designed to turn on only above a temperature of 50°C in the stack (as detected by thermistors in the stack), with a maximum allowable temperature of 65°C. The following temperature patterns were recorded for the TMDC for cooling factors of 110 W/K as designed, and 30 W/K for comparison.

Figure 4.15 Stack temperature as a function of time in TMDC

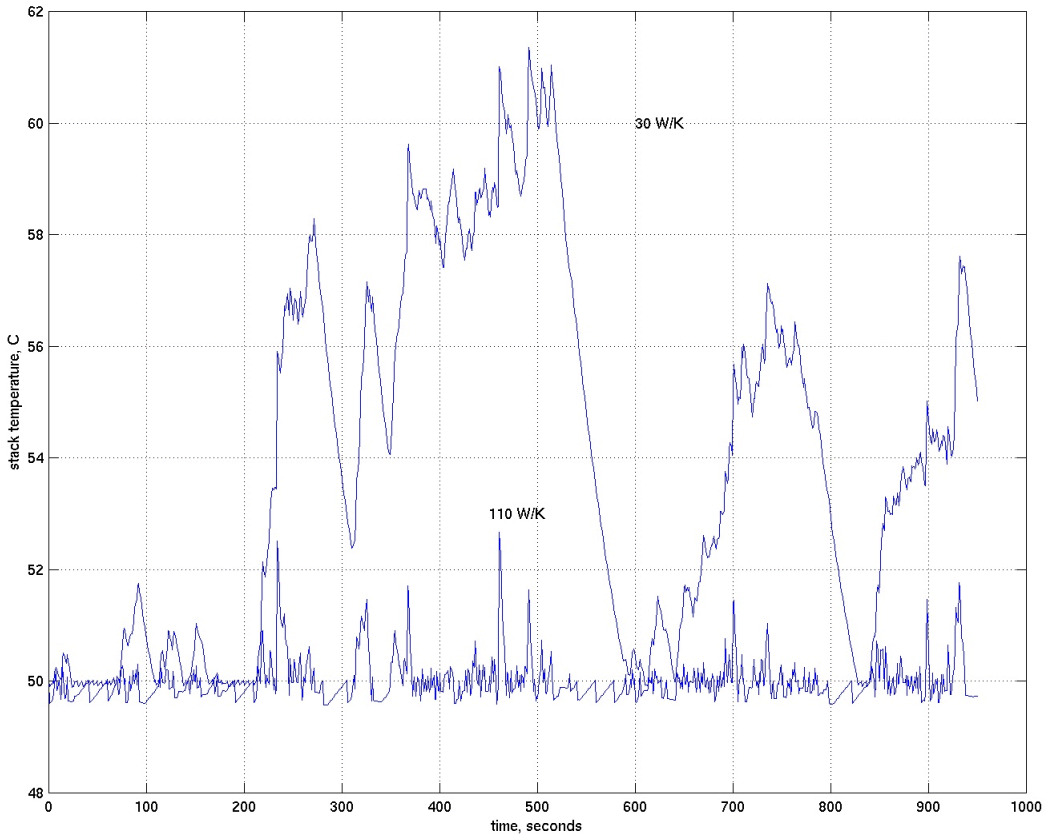

The smaller cooling factor is perfectly adequate to keep the maximum temperature below 65°C but, as calculated previously, the full 110 W/K is needed for sustained hill climbing.

As discussed, either the cooling fan or the pump could be switched on and off to produce cooling. In practice, the pump should be the unit controlled, because some cooling is still derived from pumping the water through the externally-exposed radiator, even if the fan blowing over the radiator is off. This seems like a benefit, except that excessive cooling would lower the fuel cell stack temperature below its designed operating point of 50°C; also, when the fuel cell is first started, it needs to warm up as quickly as possible.

A more sophisticated temperature simulation would include a time lag between the temperature measurement inside the stack and the control (turning the pump on or off). A more sophisticated *design* would vary the pump speed in order to reduce the power taken up by the pump, especially since adequate control could be maintained at just 20 W/K to achieve the result graphed above. This would decrease parasitic load and extend range, but, again, this was not assumed here due to the uncertainty in actual cooling power needs.

4.4.4.4 Selection

To achieve the upper limit of 110 $W \bullet K^{-1}$, a Lytron M14-120 radiator was selected. The cooling system includes a metal heat exchanger, pump operating at 1 gallon per minute (0.06 L/s), and fan blowing over the heat exchanger. For 110 $W \bullet K^{-1}$ of cooling, a fan speed of 375 cubic feet per minute (cfm) is necessary.[33]

According to performance charts (Appendix C), the coolant pressure drop in the radiator is 1.0 psi, while the fan-blown air decreases in pressure by 0.16 inches of water (40 Pa). Assuming a 50% pump efficiency and 50% fan efficiency, these translate into power demands of 25 W for the pump and 14 W for the fan. (Note that this takes the 1.0 psi coolant water pressure drop in the radiator and adds an estimated 2 psi drop from the fuel cell cooling cell flow fields)

It might seem that air supplied by ram-effect from the motion of the scooter would be enough to cool the exchanger. This is true in most cases, making the heat exchanger fan speed conservative, but false for the case of low-speed hill climbing, where power demands are high but air speed low. The design is also conservative because parasitic power is calculated as if the pump were on all the time, whereas this is actually not true as discussed previously.

This heat exchanger weighs 8.9 kg and takes up 15.2 L of space, including the fan, and accounts for a significant fraction of the total weight and volume.

4.4.5. Overall parasitics

Note that the specifications for pumps and blowers and radiators are for industrial, and often stationary, AC power components. This was done to get an idea of real world performance and cost without designing specifically for the scooter application. In practice, DC components would be needed to avoid an expensive DC-to-AC inverter, and components could likely be optimized for the application at hand. Prices, described in Chapter 5, are retail; cost to the scooter manufacturer would be as little as a quarter of retail.

The system requires a blower to push the air in, but omits the bulkier compressor and possibility of expander motor power recovery at the exhaust of the fuel cell.

The maximum parasitics estimated for the scooter system are 25 W for the coolant pump and 14 W for the fan blowing over the radiator, as discussed previously, plus a power draw from the Ametek blower power which is assumed to scale linearly with flow rate (i.e. power), from a minimum of 50 W of power at no load to 200 W at maximum fuel cell output of 6 kW. The power is calculated as if the pump and fan were on all the time, with the blower always requiring 50 W, for a total parasitic load of 89 W – 239 W over the output range of the fuel cell; in practice, power is saved by turning off – or slowing down – the fan and pump when not used.

The results are compared with those obtained by a study published by the Schatz Energy Research Center.[34] The Schatz report calculates the following total parasitic power requirements for a

nominal 4 kW vehicle (“Personal Utility Vehicle” - i.e. golf cart) fuel cell stack operating at atmospheric pressure.

In the Schatz system, the parasitic power comes from the water coolant pump, atmospheric-pressure blower, and the cooling fans. The system operates at approximately 40°C, and the air flow rate at 1.74 kW is 4.48 cfm (approximately 60% higher at the same power than the system presented here). So parasitic demands vary from 100% of gross power down to 5% above 2000 W, a fairly small fraction.

Figure 4.16 Parasitics as a function of power

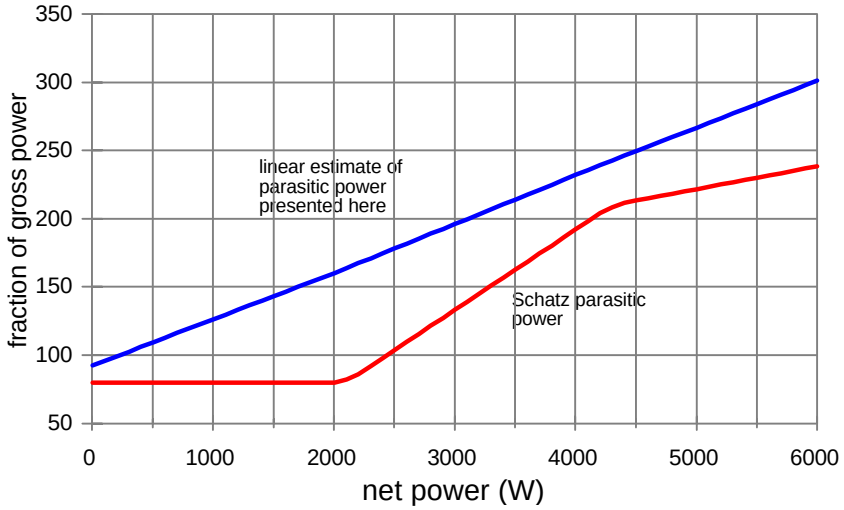

The next graph compares power usage as a percentage of gross power for both systems.

Figure 4.17 Parasitics as a percentage of power

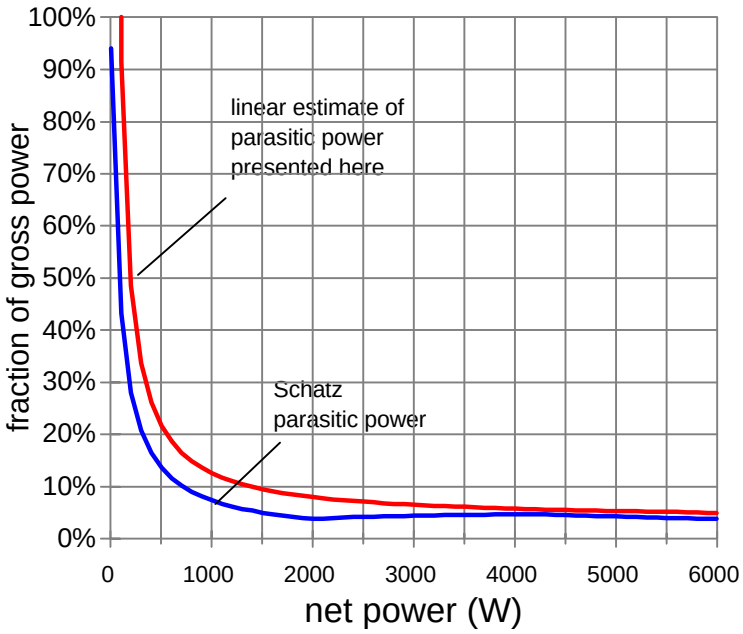

Finally, the parasitic power reduction is represented as a voltage reduction in the polarization curve. The result is a combined efficiency that has *net* electricity output as its numerator. The peak efficiency point is shifted to higher current densities and efficiency is reduced below 50% at all points.

Figure 4.18 Effect of parasitics on efficiency

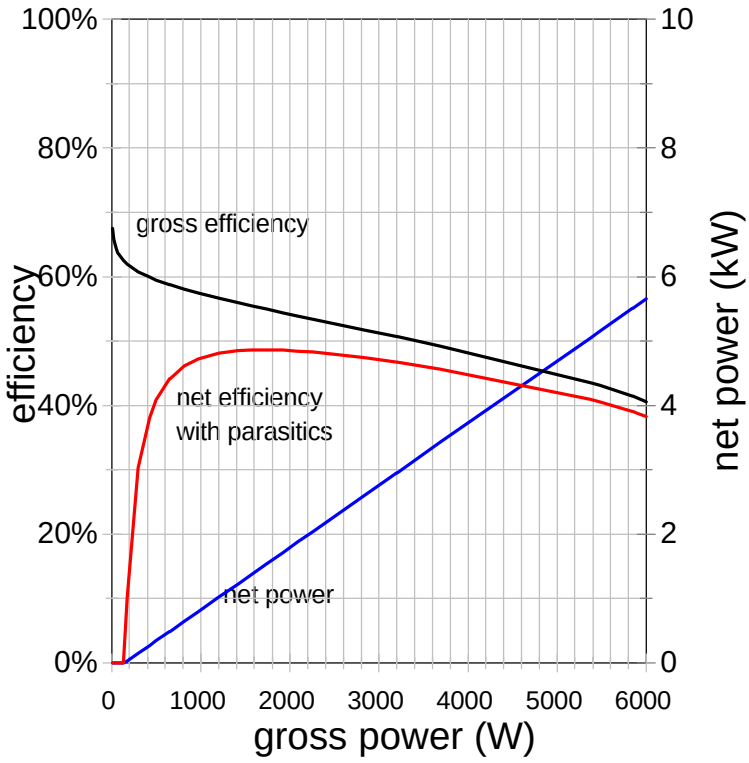

4.5 Integrated Model

4.5.1 System performance

The complete model takes the vehicle physical model described at the beginning of this chapter, and integrates the efficiency of the motor/controller subsystem, parasitic power demands, and the fuel cell polarization curve to determine overall efficiency: the amount of hydrogen consumed for a given travel distance under both the Taipei Motorcycle Driving Cycle and steady state 30 km/h driving conditions. The overall performance is used to identify the sizing of subcomponents like the fuel

storage supply and thus to determine the overall system weight and size.

Essentially, the driving cycle model is run, and at each discrete point in time, the power needed at the wheels is calculated and divided by the 77% drivetrain efficiency. An auxiliary power component of 60 W is added. Parasitic power is determined as a function of this total, and added. (This is an iterative process because the parasitic power is included in the total power, from which the parasitic power is calculated.)

Next, this total electrical output power is divided by the efficiency at that power demand; this efficiency is determined from the voltage on the polarization curve for the power required. The result is the amount of hydrogen consumed at the time interval, in terms of higher heating value energy units.

The results, over the driving cycle, are the maximum and average power (including parasitics); and the fuel economy in terms of hydrogen consumed per kilometer traveled. The latter is readily converted to miles per gallon of gasoline equivalent. An overall efficiency is calculated for the conversion process.

A battery-powered option is considered using the same basic model, but with no parasitic power to consider because fans, blowers, and pumps are not needed.

As before, the total scooter curb weight was set at 130 kg, and a 75 kg driver was added. Later results show that the vehicle weight is approximately the same as this assumption.

Table 4.13 System Performance under TMDC and at cruising speed

	TMDC	30 km/h cruise
Maximum power from fuel cell (includes drivetrain and parasitics)	5.91 kW	725 W
Average fuel cell output power	674 W	725 W
Overall efficiency	46.7%	58.5%
Fuel economy relative to hydrogen	0.527 km/g H_2	0.807 km/g
Equivalent "on-vehicle" fuel economy	344 mpge	522 mpge
Hydrogen storage for 200 km range	380 g	248 g
Average output power without parasitics (battery powered scooter)	566 W	614 W
Fuel economy of battery powered scooter	35.5 km/kWh	48.8 km/kWh
Battery energy storage for 200 km range	6.5 kWh	4.1 kWh

Note that these battery energies are given in terms of total energy output. The energy that must be put into these batteries is higher due to less-than-100% charging and discharging efficiency. However, this additional energy is not included here because price and performance figures for the zinc-air batteries are given in terms of energy output.

4.5.2 Size and weight of power system

The detailed analysis done in Appendix B and described in section 3.1.3.3 estimates a stack size and volume of 7.6 kg and 7.8 L respectively. This is a power density of 0.78 kW/kg and 0.76 kW/L for the stack alone, slightly less than 1996 Ballard stacks at 1 kW/L.

Assuming a factor of two extra for air and heat and water management subsystems gives power densities of 0.39 kW/kg and 0.38 kW/L. (The PNGV Technical Roadmap requirements are 0.4 kW/kg and 0.4 kW/L.[35]) That is a simple estimate;; the following paragraphs produce a more

detailed analysis of the subsystems. First, the heaviest and bulkiest subcomponents are analyzed and listed in Table 4.14. These are the blower that supplies air to the fuel cell stack, the pump that circulates cooling air, and the radiator. Prices are projected for mass production, with more details in section 5.1.3.

Table 4.14 Subcomponent summary

	Brand	Model	Dimensions (in cm)	Size	Weight	Cost (long term)
Fuel cell stack	–	–	–	7.8 L	7.6 kg	$220
Starter battery	Yuasa	GRT YT4L-BS	11 x 7 x 9	0.7 L	1.3 kg	$10
Coolant pump	generic	–	8 x 12 x 12	1.2 L	1 kg	$20
Radiator with fan	Lytron	M14-120		15.2 L	8.9 kg	$60
Blower	Ametek	116638-08	15 diameter x 17 length	2.9 L	2.7 kg	$110
plumbing, wiring, etc.	generic	–	–	2.0 L	3.0 kg	$50
coolant water	–	–	–	–	0.64 kg*	–
TOTAL STACK WITH AUXILIARIES	–	–	–	29.8 L	24.6 kg	$470

The "generic" pump has pressure requirements of 2.5 psi and a pumping flow rate of 1 gallon per minute. This is adequately supplied by an aquarium-type pump. Electric cabling, air manifolds, water plumbing were estimated to add 3 kg and 2 L and a cost of $100

*Note that the radiator holds 320 mL of water when full, and with an estimated total of twice that amount of water in the entire system, this adds an additional 0.64 kg of weight.

The total performance figures for the stack with auxiliaries are 0.24 kW/kg and 0.20 kW/L. The stack proper takes up 27% of the mass and 26% of the volume.

In comparison, the overall fuel cell stack weight of the Schatz 4 kW system described previously was 75 lbs or 34 kg; the entire power system weighed 200 lbs or 90 kg. Stack volume was 10" x

11" x 21", or 39 L.[36] With the greater room of a golf cart, engineering for minimum volume is not so critical, but these results still indicate that reduced size and weight have not yet been demonstrated

The sizes and weights with the hydrogen storage system included are listed in Table 4.15 below. Both a current Ergenics metal hydride system and predicted FeTi performance are included, along with a Dynetek cylinder and the ZES-2000 battery-powered scooter for comparison purposes.[37]

Table 4.15 Size of various storage designs

storage system	energy stored	range at 30 km/h (km)	range under TMDC (km)	energy storage (battery or H_2)		complete drive system	
				weight	volume	weight	volume
ZES-2000 lead-acid batteries	1.34 kWh	60	40*	44 kg	15 L	60 kg	24 L
DTI TiFe hydride	250 g H_2	200	132	21 kg	4 L	61 kg	43 L
Ergenics hydride (aluminum body)	204 g H_2	165	108	27 kg	14 L	67 kg	53 L
Dynetek cylinder (compressed gas)	350 g H2	282	184	11 kg	31 L	51 kg	70 L

"complete drive system" refers to the motor and controller from Table 2.2 (15.5 kg and 9.1 L together), the fuel cell stack, auxiliaries, and hydrogen storage.

* Note that the ZES-2000 can not actually sustain the TMDC, as it lacks the power necessary for the high-speed accelerations; its range is given as if it had could produce the required maximum *power* using its current batteries. For comparison, according to an unspecified pattern of "urban driving", it is listed at a range of approximately 30 km; reported data shows that it reaches 80 km on a single complete discharge at 30 km/h.[38]

Also, although the ZES-2000 does not actually use the Unique Mobility motor / controller system specified, these numbers are similar to those of other motor/controller systems and were used in calculating total size and weight for the battery-powered scooters.

This comparison has used the criteria of size and weight, but it should also be noted that cooling loads are higher for compressed gas hydrogen storage systems, due to the lack of desorption cooling. This results in larger cooling loads and higher parasitic demands from the cooling system, not shown here. The results of Table 4.15 are discussed in the subsection following.

4.5.3 Evaluation

Average two-stroke scooters weigh 70 kg and up, but the overall ZES-2000 prototype mass is 105 kg. A Honda CUV-ES electric scooter weighs 130 kg. Fuel cell powered scooters would weigh about as much as the CUV-ES; recall that one of the concerns in the consumer satisfaction survey was the extra weight of the electric scooter. While this might remain an item of difficulty in terms of handling while the system is off, the extra performance provided by the 6 kW fuel cell system partially compensates for the high mass.

The fuel cell vehicle offers more than three times the range of the ZES-2000, with roughly the same weight of drive system. The fuel cell systems requires 18 to 36 additional liters of storage space over that of the ZES-2000. There is a helmet storage chamber in the design that could be commandeered for additional fuel storage; this is approximately 10-15 L of space. Additional volume would have to come from a redesigning of the scooter body to make more room available, but note that current electric scooters already use redesigned large-capacity bodies.

Current laboratory-scale metal hydrides, as exhibited by the Ergenics system, are almost 30 L larger than the ZES-2000 power system, so progress must be made in improving metal hydride technology.

The following charts describe the breakdown of size and weight for the various subsystems, for a

FeTi hydrogen storage system

Figure 4.19 Weights of subsystems

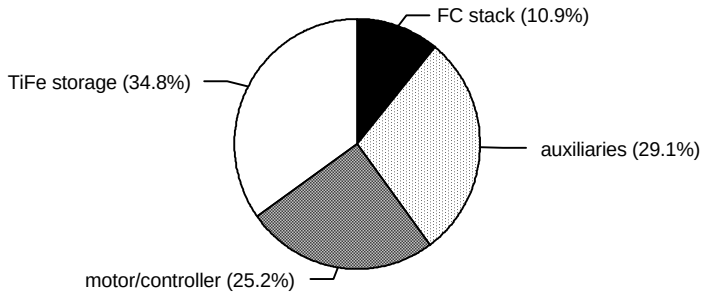

Figure 4.20 Volumes of subsystems

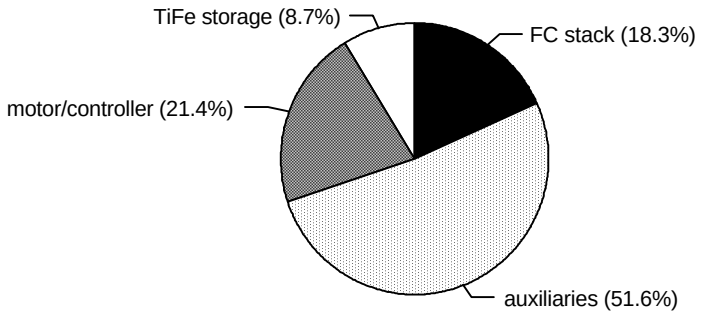

A subsequent chapter deals with the costs of the various systems, but the next section is a discussion of whether operating the fuel cell at higher pressures (with consequent greater efficiency) might improve performance and reduce the size of the fuel cell required.

4.6 Pressurized fuel cell option

One of the two options considered for improving the performance of the base design was to operate the fuel cell above atmospheric pressure. To quantify this benefit, the higher voltage output obtainable was compared to the additional power needed to drive the compressor. Also included was the fact that a turbine running of the fuel cell exhaust would reduce the compressor load. Calculations were based on a adiabatic, non-isentropic system with the 68% efficiency assumed previously.

Power out for an *adiabatic* expander (or compressor):

$$P_{adiabatic} = \dot{n}\int_{P_1}^{P_2} V\ dP = \dot{n}RT\,\frac{\gamma}{\gamma-1}\left(\left(\frac{P_1}{P_2}\right)^{\frac{\gamma}{\gamma-1}} - 1\right)$$

$\dot{n}$ is the flow rate in moles•s^{-1}; R is universal ideal gas constant, 8.314 J·mol^{-1}·K^{-1}. The specific heat ratio γ is the ratio of C_p to C_v for the working fluid. Assumptions: the intake air is an ideal gas consisting of nitrogen and 20.95% oxygen; the exhaust (mainly nitrogen, with some water vapour and unused hydrogen) is an ideal gas with the stoichiometric amount of oxygen removed by the fuel cell reaction, and no water vapour.

The benefit of compression is calculated using the two Energy Partners polarization curves discussed previously (3 atm and atmospheric). The atmospheric power is net of blower parasitic power, which is a linear function from 50 W to 250 W over the 5.9 kW operating range of the fuel cell stack. The pressurized stack power is net of compressor and expander powers, as calculated for a 68% efficiency expander and 68% efficient compressor. (same as the DOE's projected automotive

system). Note that this fails to capture the lowered efficiency expected at lower-than-nominal flow rates, while the blower's linear function does effectively reduce efficiency at low flow rates.

The mechanical power required by the compressor is always greater than the mechanical power recovered by the expander, and any supplement is calculated to be made up from the fuel cell at a 90% conversion efficiency from electricity to shaft power through an electric motor.

The figure below compares the power outputs at given current densities. Note that the powers, here, are proxies for efficiency because at a given current density both options are operating on the same amount of hydrogen per second.

Figure 4.21 Atmospheric power versus 3 atm power

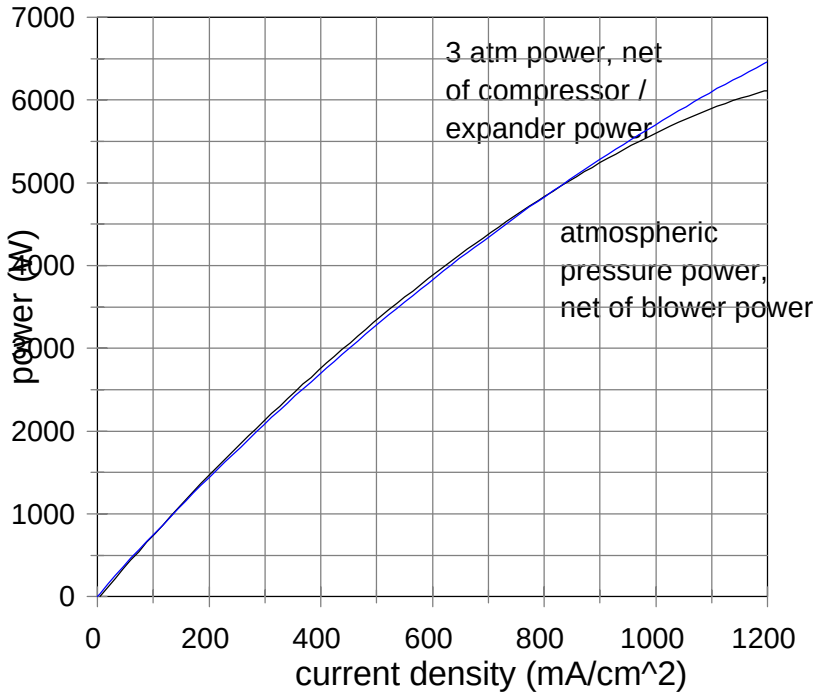

The difference expands to 350 W at 1200 A•cm^{-2}, so the pressurized fuel cell does have benefits at high pressure. However, at the maximum operating point of 1000 A•cm^{-2}, the advantage of the 3 atm fuel cell is only 105 W, or 1.8% of the gross power. Although there is an unquantified benefit for the pressurized fuel cell due to the lesser need for humidification and easier water removal, the gain is quite limited and the scooter cannot accept the additional cost and weight of an additional turbocompressor system. Also, unlike the case for automobiles, the fuel cell stack size would not be appreciably reduced by operating at 3 atm.

If the DOE goals of 3 kg and 4 L for a turbocompressor can be realized, and efficiency is good at the under-10 g/s flow rates required in scooters, then the slight performance benefit will be worth a small price premium.

4.7 Hybrid option design

A second optimizing option was considered. Due to the extremely irregular nature of scooter driving, with average power only 8% of maximum power, peaking power provided by a secondary power device might be an efficient way to reduce the fuel cell size. The fuel cell would provide baseload power and charge up the secondary (peaking) power source for later use. A peaking power device, which could be an advanced high-power battery, an ultracapacitor, or a flywheel, would also enable regenerative braking.

The targets of hybridization, for the scooter are to:

1. Reduce system cost by reducing fuel cell size; *peaking power* batteries are cheaper than additional fuel cell capacity, at least for the next several years.

2. Increase total fuel economy with regenerative braking and lower curb weight. For the same hydrogen storage, greater fuel economy means greater range.

3. Improve vehicle handling by reducing curb weight.

The major drawback is that hybrid systems require more complex controls and power conditioning systems. To optimize the system, a balance must be struck between secondary power source size and main power source size. An important consideration is whether weight and volume of auxiliaries will decrease significantly if a smaller fuel cell is used.

4.7.1. Types of hybrids

There are several types of hybrid vehicle designs. Most of these are defined for internal combustion engines and used for the purposes of (i) increasing engine efficiency, (ii) reducing emissions, and (iii) reducing cost if the main engine is expensive, like a fuel cell. Hybrids are divided into parallel and series systems.

For a combustion hybrid, a parallel system allows both the engine and the peaking battery (via electric motor) to drive the wheels using two separate systems. This system is more mechanically complex due to the two driveshaft attachments, but allows simultaneous use of the battery and the combustion engine.

In contrast, a series hybrid routes all power electrically. The combustion engine drives a generator (not required in the parallel version), which can supply energy to the wheels and the peaking battery. Output from the generator and the peaking battery go to the wheels. Generally, the engine can be set to operate only at its most efficient speed, recharging the battery as needed and avoiding transients which might produce more emissions.

The more specific operating policies listed below are from the DOE HEV program guidelines.[39] The word "battery" is used interchangeably with "secondary energy storage system," although this system could actually be a flywheel or ultracapacitor.

1. *Thermostat series*. The vehicle is run on battery power by default, with the primary power source activated (at the optimum power level) when the battery drops below a predefined minimum. The primary power source acts as a thermostat, turning on and off to maintain battery state of charge. This policy allows the primary power source to run at its peak efficiency point.

2. *Electric-assist parallel.* The primary source provides power by default, and the battery is discharged only in high-power situations. The battery is recharged by regenerative braking, but in the case of combustion engine hybrids, cannot be recharged by the engine because there is no generator. The primary power source can be sized below the maximum power required since it is assisted by the battery.

3. *Primary power-assist parallel.* Identical to the previous system, but with the battery providing power, and the internal combustion engine supplying peaking power. Very similar to a "range-extender" system in that the battery functions as the main energy storage device.

4. *Load-leveler series.* The average power is matched to the output of the primary power source, while logic attempts to maintain the state of charge of the battery at a predefined medium level. Peaking power is supplied by the battery, but the primary power source load is allowed to vary as well to maintain the state of charge of the battery. (This contrasts with the thermostat series option, where the combustion engine stays at its optimal point).

The different policies show that the design is motivated by a desire to keep the combustion engine at its optimum point (maximizing fuel economy and minimizing emissions) for the series options, and reducing the engine size in the parallel options.

A fuel cell hybrid is technically a series hybrid because there is a single drive system (electric). The fact that all power is electric means that, if designed properly, the control logic can allow both fuel cell and battery to drive the wheels (like an electric-assist parallel), or let the fuel cell recharge the battery (like a load-leveler series). Several axes of optimization remain - for example, how large to make the fuel cell, when to use the battery and when to recharge it, and how large to make the battery.

4.7.2. Fuel cell sizing

In order to calculate how to divide the power needs between the fuel cell and the battery, two criteria were specified. First, maximum power (5.6 kW net of parasitics) had be sustained for at least ten seconds. Users would be very disappointed to find that, after a few seconds of pushing their scooters to the maximum output, power started to fall off because the battery was used up. Second, the scooter had to sustain - indefinitely - the slope-climbing requirements. In other words, it had to generate enough power to climb a 12° slope at 18 km/h.

The physical model showed that these results can be obtained with a fuel cell stack with a maximum output of 3.2 kW gross power (3.0 kW net). Total cell active area was reduced by reducing the area of each cell to 110 cm^2, while the number of cells was kept the same in order to retain the 48 V motor voltage. To reach the maximum power *output* level thus required the addition of a 2.6 kW peaking battery. This is the first hybrid scooter case.

One other case was considered. This one is targets the short term where fuel cells are extremely expensive and the fuel cell size must be minimized at all costs: a fuel cell sized to output only 1.0 kW of net power (1.1 kW gross power), with a large battery for the remaining 4.6 kW.

This scooter would not be capable of indefinitely sustaining hill climbing as specified at the beginning of the chapter. The specified performances can only be achieved for under three minutes until the batteries drain down to their 20% limit, and the continuously sustained hill climbing speeds are lower than the requirements, as shown in the table below.

Table 4.16 Hybrid 1.1 kW scooter inadequacies

	15° slope	**12° slope**
Required performance	10 km/h	18 km/h
Limited amount of time at this speed as battery is drained	140 s	70 s
Limited distance at this speed	380 m	360 m
Sustainable maximum speed (after battery depleted; fuel cell only)	4.7 km/h	5.8 km/h

Cooling load is significant in hybrid vehicle design as well as in the original pure fuel cell design; again, the critical situation is hill climbing requiring 3.2 kW of continuous output. In the 5.9 kW full-sized fuel cell, continuous operation at 3.2 kW gross output takes place at 51% efficiency, and

heat production is consequently low. A 3.2 kW maximum power fuel cell, however, is only at 43% efficiency when it is continuously operated at 3.2 kW, producing more heat. The greater heat also necessitates higher pump and fan loads for the radiator, meaning greater parasitic loads.

Parasitic power loads were calculated with an iterative process. The first step was to estimate a parasitic load. Then the maximum gross output power including parasitics was calculated for hill climbing. A maximum heat output was then solved, and the parasitic power required to sustain this cooling load was calculated. The process was repeated until the results converged. In the example here, after the results had settled down to stable values, the following results were obtained:

For the first hybrid, the maximum load was 3020 W, with parasitic power costs of 66 W for pump and fan, and 50-250 W for the blower depending on load. The total fuel cell output was 3205 W at this net power output, for a waste heat load of 4240 W. With hydride cooling at 17.2% at this hydrogen flow rate, the remaining heat load was 3510 W, or 140 W/K at the pre-defined ΔT of 25°C, which was supplied by fans and pumps with the total of 66 W.

The 1.1 kW system was easier to solve because the output was simply capped at 1.0 kW of net output, because no attempt had to be made to find the total power at which the hill climbing requirements could be met. A smaller M10-080 radiator was used. Under maximum conditions of 1.1 kW gross power, heat generation was 1430 W, or 1180 W after metal hydride desorption, for a cooling load of 47 W/K.

Table 4.17 Hybrid fuel cell stack designs

	Pure FC	Hybrid 1	Hybrid 2
Maximum gross power	5.9 kW	3.2 kW	1.1 kW
Stack current at maximum power	172 A	89 A	31 A
Efficiency at maximum current density	41.2%	43.2%	43.6%
Total active area needed	9600 cm^2	5600 cm^2	2000 cm^2
Total number of fuel cells	56	56	56
Active area per cell	170 cm^2	100 cm^2	35 cm^2
Maximum fuel cell heat generation	8.4 kW	4.2 kW	1.4 kW
Maximum heat generation (after metal hydride cooling)	7.0 kW	3.5 kW	1.2 kW
Cooling factor needed at maximum power (ΔT=25°C)	280 W/K	140 W/K	47 W/K
Maximum net fuel cell power	5.9 kW	3.0 kW	1.0 kW
Battery power needed	–	2.6 kW	4.6 kW

4.7.3 Peaking battery and operating policy

The peaking power battery model is described in section 2.2.3.1 and has the following properties. Note that the specific power and power density are much higher for the battery than the fuel cells (see Table 4.24), so that hybridization makes sense in reducing total weight and volume.

Table 4.18 Peaking power battery characteristics

Specific power at 43 second discharge	836 W/kg
Specific energy	17 Wh/kg
Power density by volume	853 W/L
Energy density by volume	17 Wh/L

The heat generated by the battery is not included in the system modeling. It is on the order of 10%

of the output power, low compared to the fuel cell. At maximum output power (4.6 kW for the 1.1 kW stack hybrid) this could be almost 500 W in addition to the fuel cell, but this heat load is infrequently reached. The operating policy of the battery is defined as follows.

1. The state of charge of the battery is allowed to vary between 80% and 20% over the driving cycle. The state of charge is kept away from these "hard limits" in order to reduce the risk of large excusrions (overcharging or draining to zero), either of which could permanently damage the battery.

2. The state of charge is set at the beginning of the driving cycle is set to 50%

3. The battery is activated (discharged) whenever the fuel cell maximum power is not enough for the driving cycle power plus auxiliary and parasitic loads, and makes up the entire difference.

4. Regenerating always recharges the battery as long as the maximum charging current is not exceeded, up to the 80% limit

5. The battery is charged up from the fuel cell at a specified rate whenever (i) the state of charge dips below 55% and (ii) power demand at that instant is less than 400 W. The charging rate is equal to 400 W minus the instantaneous power demand from the wheels, auxiliaries, and parasitics.

4.7.4 Simulation results

First, fuel economy was determined under steady-state, 30 km/h driving conditions.

Table 4.19 Hybrid performance at 30 km/h

Parameters	5.9 kW pure FC	3.2 kW hybrid	1.1 kW hybrid
fuel cell conversion efficiency	58.5%	56.4%	50.0%
average fuel cell output power	725 W	751 W	710 W
fuel economy in terms of hydrogen	0.807 km/g	0.751 km/g	0.703 km/g
"on-vehicle" fuel economy	522 mpge	486 mpge	455 mpge
change from pure FC	–	-4%	-15%
hydrogen for 200 km	248 g	266 g	284 g

Efficiency decreased as the fuel cell size decreased, because the smaller fuel cells were operating closer to their maximum output. For the results below, the hydrogen storage system was scaled linearly to keep range at 200 km. The driving cycle was more interesting because its decelerations created the possibility of regenerative braking.

Table. 4.20 Hybrid performance under TMDC

Parameter	5.9 kW pure FC	3.2 kW hybrid	1.1 kW hybrid
Fuel cell maximum power	5.91 kW	3.24 kW	1.11 kW
Battery maximum power needed	–	2.61 kW	4.63 kW
Average total power output, battery + fuel cell	674 W	709 W	726 W
Average fuel cell power	674 W	698 W	577 W
Fuel economy (mpge)	344	316	343
Change in fuel economy	–	-8.2%	-0.3%
Overall conversion efficiency	56%	53%	47%
Braking energy absorbed	–	62 kJ	82 kJ
Average power absorbed	–	65 W	86 W
Braking energy recovered as a fraction of theoretical maximum braking losses	–	51%	68%

The 1.1 kW fuel cell puts out 100 watts less average power than the 5.9 kW fuel cell, because the 86 W (average) that is recovered from regenerative braking can supplement the peaks. However, conversion efficiency from hydrogen heating value to electricity is lower at 47%, because the fuel cell is operating more frequently near its maximum power (minimum efficiency). More hydrogen must be used to produce the 577 W of power than if the larger, pure fuel cell were used with the same batteries. The result is a net fuel economy that is the same as the pure fuel cell.

The 3.2 kW hybrid actually consumes more power in the TMDC due to the higher parasitic losses, and for the same reason of operation near maximum power given above.

The regenerated fractions of 51% and 68% are close to the 70% theoretical maximum that can be regenerated. The differences are due to the limiting maximum charging rate and the fact the at some points the battery is already full when regenerative braking is possible. In terms of total power, though, these figures are equivalent to 9% – 14% of the total fuel cell output.

Figure 4.22 Division of power between fuel cell and battery during TMDC, 3.2 kW stack

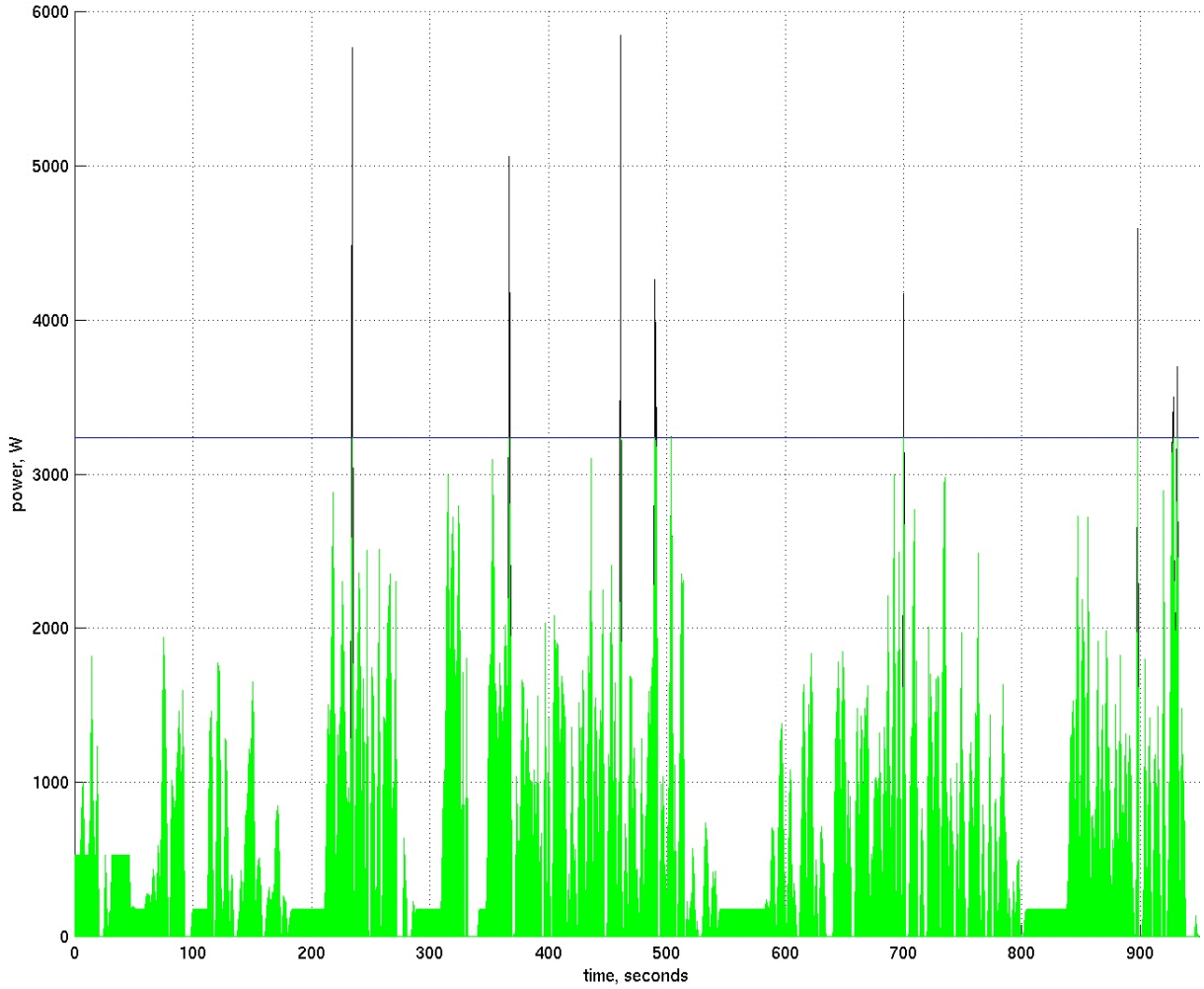

In this diagram, the dark area above the horizontal line represents the energy supplied by the peaking power battery, while the light gray area below the line is the energy supplied by the fuel cell. The same scheme is used in Figure 4.24.

Figure 4.23 State of charge of battery over TMDC, 3.2 kW stack

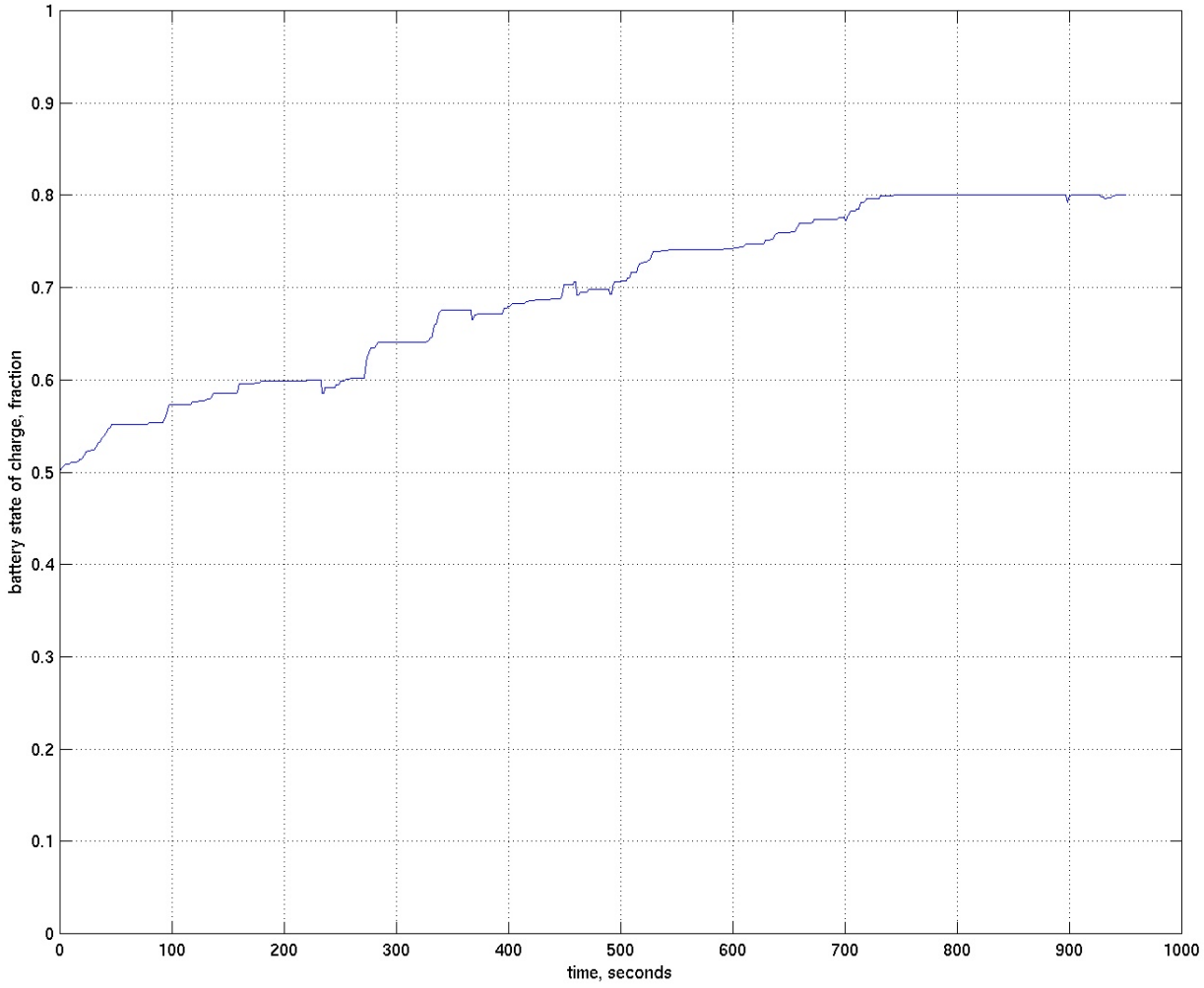

The careful observer will note that battery energy does not return to initial levels over the driving cycle - in fact, there is a net gain from regeneration of 58.3 kJ, or an average of 60 W over the 950 second cycle. There is a not insignificant amount of surplus energy that could be applied to the wheels, if the battery were employed using a more sophisticated policy (for example, using the battery even if power demand is *not* greater than the maximum fuel cell output), and fuel economy would be slightly improved.

Since the object was to minimize component cost and not necessarily produce the maximum mileage, the design of more efficient hybrid strategies will have to await future studies.

Figure 4.24 Division of power between fuel cell and battery during TMDC, 1.1 kW stack

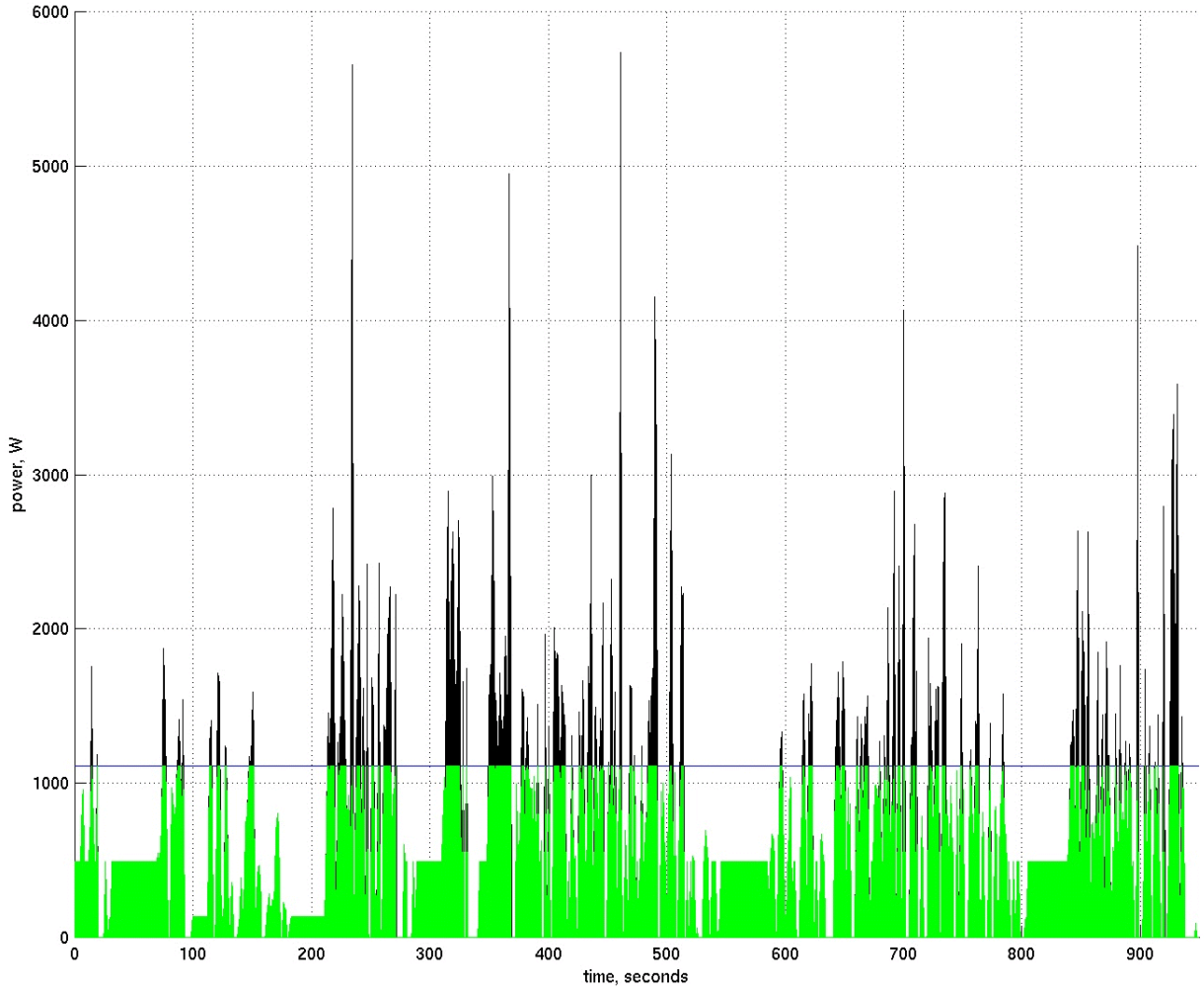

Figure 4.25 State of charge of battery over TMDC, 1.1 kW stack

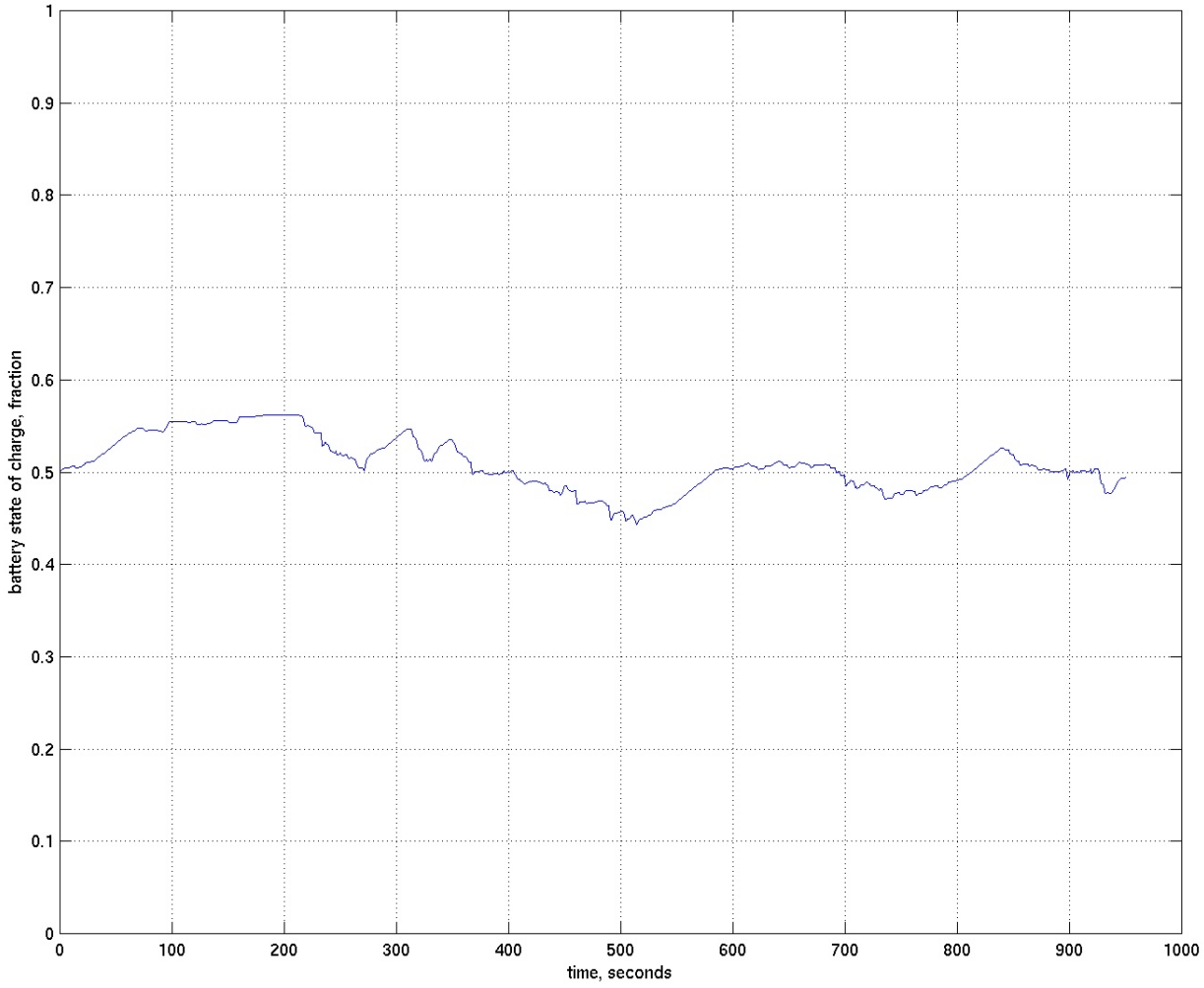

4.7.5 Hybrid power system designs

The subsystem performance requirements and sizes/weights are listed for the two hybrid designs, with the base pure fuel cell system for comparison.

Table 4.21 Hybrid system design

Parameter	5.9 kW pure FC	3.2 kW hybrid	1.1 kW hybrid
Maximum hydrogen flow rate	2.6 cfm	1.4 cfm	0.5 cfm
Maximum air flow rate	15.6 cfm	8.1 cfm	2.8 cfm
Worst-case cooling requirement	110 W/K	150 W/K	50 W/K
Cooling fan power requirement	14 W	28 W	4 W
Coolant pump power requirement	25 W	38 W	21 W
Fuel cell stack weight	6.7 kg	5.4 kg	4.1 kg
Fuel cell stack size	7.8 L	5.3 L	3.2 L
Fuel cell cost (manufacturing cost)	$220	$160	$140
Battery maximum power needed	–	2.6 kW	4.6 kW
Battery weight	–	3.1 kg	5.6 kg
Battery size	–	3.0 L	5.4 L
Battery cost (retail)	–	$195	$340

The same DTI model was used to calculate fuel cell stack sizes, weights, and costs. The designs are described in greater detail below.

4.7.5.1 Design for 3.2 kW fuel cell

For the 3.2 kW fuel cell, fuel economy actually goes down with hybridization. There are three reasons: (i) the cooling system parasitic load is larger (ii) the fuel cell is operating more frequently near its maximum load (iii) the battery is rarely used to output energy.

At maximum cooling load and 50% efficiency, the cooling fan runs at 500 cfm (0.24 inches of water pressure drop) and uses 28 W of power while the pump pushes coolant at 1 gpm (2.5 psi pressure drop) and uses 38 W. Thus, the base load power needed for the cooling system is 66 W.

The lower air intake flow requirements might make a smaller and cheaper blower feasible.

With auxiliaries the power system totals are 21.9 kg and 26.6 L, for power densities of 0.15 W/kg and 0.12 W/L.

Table 4.22 Component breakdown for 3.2 kW scooter

Component	Weight	Volume	Long-term cost
Fuel cell stack	5.4 kg	5.3 L	$165
Radiator and fan	8.9 kg	15.2 L	$60
Coolant pump	1.0 kg	1.2 L	$10
Blower	2.7 kg	2.9 L	$110
plumbing, wiring, etc.	2.0 kg	2.0 L	$50
coolant water	0.9 kg	–	–
peaking power battery	3.1 kg	3.0 L	$195
TOTAL STACK WITH AUXILIARIES	25.1 kg	29.6 L	$590
motor	11.4 kg	5.0 L	$125
controller	4.1 kg	4.1 L	$150
hydride for 266 grams H2	22.8 kg	4.0 L	$200
TOTAL DRIVE SYSTEM	63 kg	43 L	$1065

Due to the lower fuel economy of the 3.2 kW system at 30 km/h, slightly more metal hydride is needed: 266 grams for 200 km. This requires a 22.8 kg system taking up 4.0 L of space.

The total size and weight are very close to the original, 5.9 kW fuel cell. Mainly this is because the subsystem sizes remain the same even though the fuel cell proper becomes smaller. Smaller blowers and coolant pumps could be used, reducing weight slightly, but the largest subcomponent (the radiator) has to stay large in order to handle the higher cooling factor of 140 W/K.

4.7.5.2. Design for 1.1 kW fuel cell

In the second hybrid, the battery is used much more often and contributes frequently to the total power output. However, for the same reason, the battery must be frequently replenished, and due to the small size of the 1.1 kW fuel cell, the fuel cell often runs near its inefficient maximum output. The net fuel economy is almost identical to that of the pure fuel cell.

Cooling is different. The system is sized for cooling when it is running flat out at the maximum 1 kW of net output, rather than for sustained (3020 W) hill climbing. After metal hydride cooling, the worst-case cooling load is less than 50 W/K. This is achievable with a fan at 140 cfm with 0.125 inches of water air pressure drop (4 W of power), and a pump at 1 gallon per minute with 0.5 psi water pressure drop (21 W of power), for a total of 25 W. The lower cooling load of 50 W/K means that a smaller radiator can be used here – the Lytron M10-080.

With auxiliaries, the power system totals are 21.9 kg and 26.6 L, for power densities of 0.15 W/kg and 0.12 W/L.

Table 4.22 Component breakdown for 1.1 kW scooter

Component	Weight	Volume	Long-term cost
Fuel cell stack	4.1 kg	3.2 L	$135
Radiator and fan	3.1 kg	2.3 L	$30
Coolant pump	1.0 kg	1.2 L	$10
Blower	2.7 kg	2.9 L	$110
plumbing, wiring, etc.	2.0 kg	2.0 L	$50
coolant water	0.6 kg	–	–
peaking power battery	3.1 kg	3.0 L	$340
TOTAL STACK WITH AUXILIARIES	20.1 kg	17.0 L	$675
motor	11.4 kg	5.0 L	$125
controller	4.1 kg	4.1 L	$150
hydride for 285 grams H2	24.3 kg	4.3 L	$215
TOTAL DRIVE SYSTEM	60 kg	30 L	$1165

Due to the lower fuel economy of the 1.1 kW system at 30 km/h, slightly more metal hydride is needed: 284 grams for 200 km. This requires a 24.3 kg system taking up 4.2 L of space.

The extra battery size is compensated for by the smaller fuel cell, while the smaller radiator makes a large difference in reducing the total volume.

4.7.5.3 Hybrid zinc-air scooters

If fuel cells can be hybridized with peaking power batteries, why not battery powered scooters? Regenerative braking would extend the range of the vehicle, while separating the power and energy functions might allow a smaller, less expensive power system. In the fuel cell, energy and power are decoupled. The fuel cell engine is sized for a maximum power output, and the amount of hydrogen

carried can be varied to meet range requirements. With the battery, a larger power necessarily corresponds to a larger energy storage, and sizing for power may result in overdesigned energy (or vice versa). The hybrid battery system reduces this dependence by using batteries with two different power-to-energy relationships.

The hybrid battery design presented here uses zinc-air batteries (high energy density) for range, plus the peaking power lead-acid batteries (high power density) described above. The two sets of batteries operate in the same way as the fuel cell hybrid, so that the peaking power of the high power lead-acid batteries can be added to the zinc-air baseload battery's power, and the peaking batteries can be used to absorb regenerative braking energy.

The power and energy requirements are specified so that the scooter has enough power to sustain the maximum accelerations of the TMDC, and enough energy to drive 200 km at a constant speed of 30 km/h (or 145 km under the TMDC). 5.6 kW of output power and 4.1 kWh of energy storage are needed, and the following results are obtained:

Table 4.24: Hybrid battery configuration for Taiwan scooter model

Parameter	Zinc-Air baseload battery	Spiral lead-acid peaking battery	Total
Weight	20.5 kg	4.5 kg	25.0 kg
Energy Capacity	4.1 kWh	0.07 kWh	4.1 kWh
Peak Power	1.8 kW	3.8 kW	5.6 kW
Specific Energy	200 Wh/kg	17 Wh/kg	168 Wh/kg
Specific Power	90 W/kg	836 W/kg	210 W/kg
Volume	27.1 L	4.4 L	31.5 L
Long term mass-production price	80 $/kWh	75 $/kW	–
Total price	$330	$285	$615

The zinc-air volumetric energy density is calculated to be 150 Wh/L from published data; cost for high-power lead acid battery is estimated at 166 $/kW based on a scaled up version of Bolder batteries.[40] This is reduced to 75 $/kW in mass production (The Rebel battery's density is approximately 1 kg/L and the future goal is $150/kWh for long term USABC batteries and advanced lead-acid batteries. Somewhat arbitrarily, power systems are assumed to be half as expensive per kilowatt as base load batteries.[41])

Note that the continuous power output of 1.8 kW is not sufficient for the continuous hill climbing needs; rather, the baseload battery is sized for the 200 km range and 4.1 kWh required. Thus, the hybrid battery vehicle is more comparable to the 1.1 kW fuel cell system than the 3.2 kW system.

(The Electric Fuel company has its own, more conservative hybrid battery scooter theoretical design; it is specified for 4 kW maximum power and 3.0 kWh energy storage, for a claimed range of 200 km. This 3.0 kWh storage is underspecified, according to the calculations earlier in this chapter. Their power source consists of two 8 kg zinc-air batteries, each 9.9 L, 7.5 kg, and with an output of a maximum of 0.75 kW. The peaking power source must thus supply 2.5 kW, and is not described in the Electric Fuel report although it likely will be a NiCd battery.[42]

4.7.6 Hybrid results

The hybridization study reveals that peaking power batteries do not significantly reduce the mass and volume of the fuel cell system, because the auxiliary cooling and fluid management systems require a certain minimum space and mass which does not decrease rapidly with size.

Fuel economy did not improve significantly, due to the fact that with a 3.2 kW fuel cell, only a few

excursions required use of the battery and parasitic loads were higher than for the pure fuel cell. The 1.1 kW version produced fuel economies equal to the original pure fuel cell because of its lower efficiencies; on the other hand, it reduced the size of the fuel cell stack by a factor of more than five, which is important for the short term cost.

Table 4.25 Hybrid power system summary

	5.9 kW fuel cell	**3.2 kW hybrid**	**1.1 kW hybrid**	**1.8 kW battery hybrid**
ultimate stack cost	$244	$161	$124	–
stack cost/kW	$42	$47	$103	–
stack size	7.8 L	5.3 L	3.2 L	–
stack weight	7.6 kg	5.4 kg	4.0 kg	–
stack with auxiliaries, size (excl. peaking battery)	29.8 L	26.6 L	11.6 L	–
stack with auxiliaries, weight (excl. peaking battery)	24.6 kg	21.9 kg	14.6 kg	–
baseload battery (zinc-air) volume	–	–	–	27.1 L
baseload battery (zinc-air) weight	–	–	–	25.0 kg
power source power density	0.20 kW/L	0.12 kW/L	0.09 kW/L	0.07 kW/L
power source specific power	0.24 kW/kg	0.15 kW/kg	0.08 kW/kg	0.07 kW/kg

In terms of the useful performance measurements of fuel economy total power system size/weight (including fuel cell or baseload battery, peaking power battery, and hydrogen storage, but not motor and controller), the following results are obtained:

Table 4.26 Performance metrics

	5.9 kW fuel cell	3.2 kW hybrid	1.1 kW hybrid	1.8 kW battery hybrid
hydrogen storage (FeTi hydride) weight for 200 km range	21.4 kg	22.8 kg	24.3 kg	–
hydrogen storage (FeTi hydride) volume	3.7 L	4.0 L	4.3 L	–
peaking power battery weight	–	3.1 kg	5.6 kg	4.5 kg
peaking power battery size	–	3.0 L	5.5 L	4.4 L
total drive system weight	61 kg	63 kg	60 kg	45 kg
total drive system size	43 L	43 L	30 L	41 L
30 km/h fuel consumption	0.807 km/g	0.751 km/g	0.703 km/g	48.8 km/kWh
TMDC fuel consumption	0.527 km/g	0.484 km/g	0.525 km/g	36.2 km/kWh
30 km/h fuel economy	522 mpge	486 mpge	455 mpge	1053 mpge
TMDC fuel economy	344 mpge	320 mpge	363 mpge	780 mpge
Range at 30 km/h	200 km	200 km	200 km	200 km
Range under TMDC	131 km	129 km	149 km	148 km

"total drive system" includes fuel cell and hydrogen storage, or zinc-air battery; motor / controller; peaking power battery. Costs are discussed in the next chapter.

Note that the ZES drive system weight is 44 kg of lead-acid batteries plus 15.5 kg of motor and controller (assuming similar characteristics as the UQM motor/controller). This is about 60 kg, the same as the fuel cell systems.

System size does not decrease significantly with hybridization except in the case of the 1.1 kW hybrid where much lower cooling requirements mean a much smaller radiator. The smaller fuel cell weight is roughly compensated for by the added weight of the batteries, and the larger hydrogen storage tank. TMDC performance is better for the 1.1 kW hybrid because the frequent decelerations allow regenerative braking gains; the same is true for the 1.8 kW battery hybrid.

On the other hand, certain other factors decrease more or less linearly with fuel cell size, foremost among them membrane area and platinum cost. Significant cost reductions might be possible under such a system for the near future while fuel cells remain extremely expensive; unfortunately, these costs are not reflected in the price calculations above, which rely upon ultimate price estimates for mass-produced stacks.

More complex hybrid operation policies could be used to try to better predict power demands; these would optimize battery usage by controlling more cleverly when to recharge, how quickly to recharge, and the state of charge to maintain in the battery.

4.7.7 Near-term possibilities

To compare these designs with what is available today, portable stacks from H-Power and Ballard were inserted into the 1 kW fuel cell design. A single PS-250 fuel cell unit commercially available from H Power produces 250 W net power, weighs 10.3 kg, and has a volume of 16 L.[43] This does not include storage. (The system is air-cooled, and with the correct geometry this could be possible for a scooter version) The existing design can actually output 330 W; to be conservative, retail units are sold derated to 250 W. Using three units to supply the 1.0 kW net output desired produces a power system weight of 31 kg and volume of 48 L. Currently costs are on the order of $6,000 for a unit like the PS-250, with mass-production costs expected to drop to $1,000.[44] For the required three, then, the current cost would be on the order of $18,000 and $3,000 in the long run.

On the other hand, Ballard Power Systems has developed a 1 kW (net power) stack that weighs 18 kg and has a volume of 33 L including all packaging.[45]

Table 4.27: Near term 1 kW fuel cell hybrid designs

Parameter	as designed	Ballard stack	H-Power stack
fuel cell stack weight	4.1 kg	–	–
fuel cell stack volume	3.2 L	–	–
stack power density, gravimetric	95 W/kg	–	–
stack power density, volumetric	76 W/L	–	–
fuel cell system weight	14.6 kg	18 kg	31 kg
fuel cell system volume	11.6 L	33 L	48 L
fuel cell system power density, gravimetric	75 W/kg	61 W/kg	35 W/L
fuel cell system power density, volumetric	65 W/L	33 W/L	23 W/L

The fuel cell system size and weight exclude peaking power battery in all cases.

So in the short term, an unoptimized fuel cell hybrid based on Ballard performance figures would have a drive system at 63 kg and 51 L. This is 3 kg and 27 L more than the ZES-2000, which is technically feasible in a scooter.

The results here for the various types of hybrids show that they offer the opportunity to reduce fuel cell stack size and power, and thus save money, since peaking power batteries are currently cheaper (per kW) than additional fuel cell capacity. In the short term, hybrid scooters are overwhelmingly favoured. The first steps to take would be to reduce volume by optimizing the subcomponents for the scooter body.

However, in the long run, the decreasing cost of fuel cell stacks is expected to make hybrids less and less economical. A larger fuel cell also improves fuel economy at constant driving speeds, since the fuel cell is more frequently operating at its most efficient output levels.

A calculation of costs, both for the scooter and for the fuel it uses, is found in the next chapter.

Infrastructure and overall fuel economy are also discussed.

References for Chapter 4

1. Jet P. H. Shu, Wei-Li Chiang, Bing-Ming Lin, Ming-Chou Cheng. Mechanical Industry Research Laboratories, Industrial Technology Research Institute. "The Development of the Electric Propulsion System for the ZES2000 in Taiwan". (Date unknown; not the same as the SAE paper in reference 7, even though it appears to be written by the same authors. October 1997 or later.)

2. Yoshihiro Nakazawa, Chiaki Humagai, Mikio Kato. "Development of an electric scooter for practical use" in *JSAE Review* **15** (1994) 373-377

3. Chien-Tung Liu, Bing-Ming Lin, Jyh-Sheng Pan. "Design and development of a zero-emission scooter for Taiwan" in *Journal of Power Sources* **59** (1996) 185-187

4. Peter A. Lehman, Charles E. Chamberlin. "Design and Performance of SERC's Fuel Cell Powered Vehicle Fleet" in *Fuel Cell Seminar Abstracts 1998*. 714-717

5. Mowick Limited Golf & Leisure Vehicles. "E-Z Go 4Caddy" http://www.mowick.com/ezwhite.htm Accessed July 30, 1999

6. Chien-Tung Liu, C. C. Kuo, Jyh-Sheng Pan, Bing-Ming Lin. "Development of electric motor cycle technologies in Taiwan" *J. Power Sources* **48** (1994) p. 244

7. P. H. Jet Shu, Wei-Li Chiang, Bing-Ming Lin, Ming-Chou Cheng. "The Development of the Electric Propulsion System for the Zero Emission Scooter in Taiwan". (1997) SAE 972107

8. *ibid*

9. Highway Tire Committee, SAE. Revised by the Rolling Resistance Subcommittee. "Measurement of Passenger Car, Light truck and highway truck and bus tire rolling resistance" (March 1997) SAE Information Report J1270. Section 8.1

10. Frank Rowland Whitt, David Gordon Wilson. *Bicycling Science* (MIT Press: Cambridge, 1974) p. 93

11.Wei-Li Chiang, Power Machinery Division Director, ITRI-MIRL (Industrial Technology Research Institute, Mechanical Industry Research Laboratories. Personal communication, September 11 1998

12. CALSTART web site. "DARPA Consortia EV and Hybrid EV Technology Projects - (PNGV) Target Attributes" http://www.calstart.org/about/pngv/pngv-ta.html

13. Energy and Environment Analysis. "Analysis of Fuel Economy Boundary for 2010 and Comparison to Prototypes" (November 1990) Prepared for Martin Marietta Energy Systems, Contract No. 11X-SB0824.

p. 4-11.

14. M. Ross and W. Wu. “Fuel Economy Analysis for a Hybrid Concept Car Based on a Buffered Fuel-Engine Operating at a Single Point” SAE Paper 950958, presented at the SAE International Exposition, Detroit, MI, February 27 - March 2 1995

15. C. E. (Sandy) Thomas, Brian D. James, Frank Lomax, Ira F. Kuhn, Jr. Directed Technologies, Inc.“Integrated Analysis of Hydrogen Passenger Vehicle Transportation Pathways”, draft final report. For NREL, subcontract AXE-6-16685-01. March 1998. p. 61

16. Bernward E. Bayer, “Motorcycles”. Chapter 10 of *Aerodynamics of Road Vehicles*. Fourth Edition. Ed. Wolf-Heinrich Hucho. p. 502

17. Arne LaVen. “Driving Cycle Analysis of the Sun Com™ Battery Electric Scooter” (November 1998) Desert Research Institute. p. 26

18. Wei-Li Chiang, Power Machinery Division Director, ITRI-MIRL. Personal communication, September 11 1998

19. Owner’s manual for Honda CH250 Elite250 1986, (Honda Motor Company: 1985) p. 68

20. T. C. Pong, personal communication. October 29, 1998.

21. Arne LaVen. Energy and Environmental Engineering Center, Desert Research Institute. “Driving Cycle Analysis of the Sun Com™ Battery Electric Scooter” November 1998

22. Chien-Tung Liu, Bing-Ming Lin, Jyh-Sheng Pan. p. 186

23. Toshiharu Sawada, Minoru Wada, Masanori Noguchi, Buhei Kobayashi. Komatsu Zenoah Co. “Development of a Low Emission Two-Stroke Cycle Engine” SAE 980761 (1998)

24. C.T. Liu, C. C. Kuo, J. S. Pan, B. M. Lin.“Development of electric motor cycle technologies in Taiwan”

25. Christopher S. Weaver, Lit-Mian Chan.“Motorcycle Emission Standards and Emission Control Technology” Revised Final Report, submitted to The World Bank. (Engine, Fuel, and Emissions Engineering, Inc.: August 1994) page *v*.

26. Frano Barbir. Energy Partners. “Operating Pressure and Efficiency of Automotive Fuel Cell Systems” No date. 1997 or later.

27. Vicor product data sheet. “The MegaPAC family” http://www.vicr.com/pdf/ds_megapac.pdf Accessed July 9, 1999

28. Vicor sales representative. Personal communication. July 14 1999.

29. Lisa Fawcett, AMETEK. Personal communication. April 26 1999.

30. Charles Chamberlin, Schatz Energy Research Center, Personal communication. May 20 1999

31. Mazda Australia web page. “Mazda”. http://www.mazda.com.au/corpora/460.htm. Accessed June 17, 1999

32. If the entire 0.9 g/s were vaporized (with a latent heat of vaporization of 2.2 kJ/g for 100°C water) approximately 2 kW of cooling would be realized, or about 25% of the total heat generated.

33. Lytron product catalog, "Standard OEM Coils" at http://www.lytron.com/catalog/oemframe.htm. Last accessed April 11, 1999

34. Charles E. Chamberlin and Peter A. Lehman. "Design and Performance of SERC's Prototype Fuel Cell Powered Vehicle"

35. National Research Council. *Review of the Research Program of the Partnership for a New Generation of Vehicles.* Second Report (National Academy Press, Washington: 1996) p. 53

36.Susan Ornelas, Research Engineer, Schatz Energy Research Center. Personal communication February 17 1999.

37. No similar size and weight data was available for the CUV-ES scooter. Also, the Dynetek cylinder is one that holds about 40% more hydrogen than the DTI model, as no Dynetek cylinder currently exists for the designed 250 gram size.

38. Jet P. H. Shu *et al*, "The Development of the Electric Propulsion System for the ZES2000 in Taiwan"

39. Department of Energy Hybrid Electric Vehicle Program. "Energy Management and System Control". http://www.hev.doe.gov/components/energman.html. Accessed May 10, 1999.

40. Bolder "Rebel" battery pack product sheet; see specifications in section 2.2.3.1

41. ALABC [Advanced Lead-Acid Battery Consortium] web site. "About ALABC" http://www.alabc.org/about.html

42. Jonathan Whartman, Ian Brown. Electric Fuel, Ltd. "Zinc Air Battery-Battery Hybrid for Powering Electric Scooters and Electric Buses" November 1, 1998

43. Rene Dubois, H Power. Personal communication June 7 1999

44. Arthur Kaufman, H Power, personal communication May 21 1999

45. Ballard product data sheet. "1 kW fuel cell generator"